CRISPR-based platform for multimodal genetic screens in human iPSC-derived neurons

Ruilin Tian[1,2,3,6], Mariam A. Gachechiladze[4,6], Connor H. Ludwig[1,3,6], Matthew T. Laurie[1], Jason Y. Hong[1,3], Diane Nathaniel[1,3], Anika V. Prabhu[5], Michael S. Fernandopulle[4], Rajan Patel[4], Michael E. Ward[4,*], Martin Kampmann[1,3,7,*]

[1]Institute for Neurodegenerative Diseases, Department of Biochemistry and Biophysics, University of California, San Francisco, San Francisco, CA 94158, USA

[2]Biophysics Graduate Program, University of California, San Francisco, San Francisco, CA 94158, USA

[3]Chan-Zuckerberg Biohub, San Francisco, CA 94158, USA

[4]National Institute of Neurological Disorders and Stroke, National Institutes of Health, Bethesda, MD 20892, USA

[5]National Institute of Childhood Health and Human Development, National Institutes of Health, Bethesda, MD 20892, USA

[6]Co-first author

[7]Lead contact

*Correspondence: wardme@nih.gov (M.E.W), martin.kampmann@ucsf.edu (M.K.)

SUMMARY

CRISPR/Cas9-based functional genomics have transformed our ability to elucidate mammalian cell biology. Most previous CRISPR-based screens were conducted in cancer cell lines, rather than healthy, differentiated cells. Here, we describe a CRISPR interference (CRISPRi)-based platform for genetic screens in human neurons derived from induced pluripotent stem cells (iPSCs). We demonstrate robust and durable knockdown of endogenous genes in such neurons, and present results from three complementary genetic screens. First, a survival-based screen revealed neuron-specific essential genes and genes that improved neuronal survival upon knockdown. Second, a screen with a single-cell transcriptomic readout uncovered several examples of genes whose knockdown had strikingly cell-type specific consequences. Third, a longitudinal imaging screen detected distinct consequences of gene knockdown on neuronal morphology. Our results highlight the power of unbiased genetic screens in iPSC-derived differentiated cell types and provide a platform for the systematic dissection of normal and disease states of neurons.

KEYWORDS

CRISPR interference; CRISPRi; functional genomics; neuron; stem cell; essential genes; CROP-Seq; single-cell RNA-sequencing; high-content microscopy; morphology

INTRODUCTION

One of the most profound puzzles in biology is how the human genome, with only ~20,000 protein-coding genes, can provide the blueprint for a highly complex organism with hundreds of distinct cell types interacting in tissues and organs. The discrepancy between the number of human genes and the complexity of the human body is highlighted by the brain, arguably the most complex organ in the body, which comprises ~100 billion neurons connected by approximately one quadrillion synapses. In contrast, the genome of budding yeast, a vastly simpler unicellular organism, still contains ~6,600 protein-coding genes. Thus, the number of genes in the human genome, merely three times the number of genes in yeast, cannot account for the astounding difference in complexity between humans and yeast.

The challenge of encoding biological complexity in multicellular organisms may have been solved, in part, by diversifying the functions of individual genes across cell types. Thus, the same gene product can be repurposed for different cell-type specific tasks. For example, activation of c-Jun N-terminal kinase (JNK) regulates apoptosis in some cell types, but proliferation in others (Smith et al., 1997). Furthermore, mutations in broadly expressed genes, including housekeeping genes, can cause remarkably cell-type specific defects and disease states. Striking examples are familial mutations that cause neurodegenerative diseases: While many of these mutations are in widely expressed genes, distinct neuronal subtypes are selectively vulnerable in neurodegenerative diseases.

Therefore, to understand the function of the human genome, we must characterize the roles of genes in specific cell types. A powerful approach to functionally annotate the human genome is genetic screening in cultured cells. The robustness of such screens has improved substantially through the recent introduction of CRISPR/Cas9-based approaches. Cas9 nuclease can be targeted by single guide RNAs (sgRNAs) to introduce DNA breaks in coding regions of genes, which are subsequently repaired by non-homologous end-joining pathways. This process frequently causes short deletions or insertions that disrupt gene function. This CRISPR nuclease (CRISPRn) strategy has enabled genetic screens through the use of pooled sgRNA libraries targeting large numbers of genes (Koike-Yusa et al., 2014; Shalem et al., 2014; Wang et al., 2014; Zhou et al., 2014). We previously developed an alternative platform for loss-of-function screens in mammalian cells based on CRISPR interference (CRISPRi) (Gilbert et al., 2014). In CRISPRi screens, sgRNAs target catalytically dead Cas9 (dCas9) fused to a KRAB transcriptional repression domain to transcription start sites in the genome, thereby inhibiting gene transcription. CRISPRn and CRISPRi screening platforms each have their advantages for specific applications (Kampmann, 2018; Rosenbluh et al., 2017), but generally yield similar results (Horlbeck et al., 2016). Most previous CRISPR-based screens were implemented in cancer cell lines or stem cells rather than healthy differentiated human cells, thereby limiting potential insights into cell type-specific roles of human genes.

Here, we present a CRISPRi-based platform for genetic screens in human induced pluripotent stem cell (iPSC)-derived neurons, which we developed to address this need. To our knowledge, it is the first description of a large-scale CRISPR-based screening platform in any differentiated, human iPSC-derived cell type. We focused on neurons as our first application, since the functional genomic screens in human neurons have the potential to reveal mechanisms of selective vulnerability in neurodegenerative diseases (Kampmann, 2017) and convergent mechanisms of neuropsychiatric disorders (Willsey et al., 2018), thus addressing urgent public health issues. iPSC technology is particularly relevant to the study of human neurons, since

primary neurons are difficult to obtain from human donors, and non-expandable due to their post-mitotic nature.

We integrated CRISPRi technology with our previously described i^{3}Neuron platform (Fernandopulle et al., 2018; Wang et al., 2017), which yields large quantities of highly homogeneous neurons, which are needed for robust population-based screens. We decided to use CRISPRi rather than CRISPRn, since CRISPRn-associated DNA damage is highly toxic to iPSCs and untransformed cells (Haapaniemi et al., 2018; Ihry et al., 2018). Furthermore, CRISPRi perturbs gene function by partial knockdown, rather than knockout, thereby enabling the investigation of the biology of essential genes.

We then demonstrate the versatility of our approach in three complementary genetic screens, based on neuronal survival, single-cell RNA sequencing, and neuronal morphology. These screens revealed striking examples of cell-type specific gene functions and identified new genetic modifiers of neuronal biology. Our results provide a strategy for the systematic dissection of normal and disease states of neurons, and highlight the potential of interrogating human cell biology and gene function in iPSC-derived differentiated cell types.

RESULTS

Robust CRISPR interference in human iPSC-derived neurons

As a first step towards a high-throughput screening platform in neurons, we developed a scalable CRISPRi-based strategy for robust knockdown of endogenous genes in homogeneous populations of human iPSC-derived neurons. We built on our previously described i^{3}Neuron (i^{3}N) platform, which enables large-scale production of iPSC-derived glutamatergic cortical neurons. Central to this platform is an iPSC line with an inducible Neurogenin 2 (Ngn2) expression cassette (Zhang et al., 2013) in the AAVS1 safe-harbor locus (Fernandopulle et al., 2018; Wang et al., 2017). To enable stable CRISPRi in iPSC-derived neurons, we generated a plasmid (pC13N-dCas9-BFP-KRAB) to insert an expression cassette for CAG promoter-driven dCas9-BFP-KRAB into the CLYBL safe harbor locus (Cerbini et al., 2015) (Fig. 1A). We then integrated this cassette into our i^{3}N iPSC line, and called the resulting monoclonal line CRISPRi-i^{3}N iPSCs. A normal karyotype was confirmed for CRISPRi-i^{3}N iPSCs (Supplemental Fig. S1A).

To validate CRISPRi activity, we transduced these iPSCs with a lentiviral construct expressing an sgRNA targeting the transferrin receptor gene (*TFRC*). Knockdown of *TFRC* mRNA, as quantified by qRT-PCR, was robust in iPSCs and in i^{3}Neurons for several weeks after differentiation (Fig. 1B). We also characterized knockdown of two additional genes, *GRN* and *CDH2* (encoding progranulin and N-cadherin, respectively), at the protein level in differentiated neurons. Immunofluorescence microscopy showed robust knockdown of these genes (Fig. 1C and Supplemental Fig. S1B). Our platform thus enables potent CRISPRi knockdown of endogenous gene expression in i^{3}Neurons, which can be produced in the large numbers required for forward genetic screens.

A pooled CRISPRi screen reveals neuron-essential genes

We then used this platform to identify cell type-specific genetic modifiers of survival in pooled genetic screen in iPSCs and iPSC-derived neurons (Fig. 2A). We first transduced CRISPRi-i^{3}N iPSCs with our lentiviral high-complexity sgRNA library H1 (Horlbeck et al., 2016). The H1 library targets 2,325 genes encoding kinases and other proteins representing the “druggable

genome" with at least five independent sgRNAs for each gene, plus 500 non-targeting control sgRNAs, for a total of 13,025 sgRNAs. Transduced iPSCs were either passaged for 10 days, or differentiated into neurons by doxycycline-induced *Ngn2* expression. Neurons were collected 14, 21 and 28 days post-induction. Frequencies of cells expressing each sgRNA at each time point were determined by next-generation sequencing of the sgRNA-encoding locus. We observed highly correlated sgRNA frequencies between experimental replicates (Supplemental Fig. S2A), supporting the robustness of these measurements.

To analyze the screen results, we developed a new bioinformatics pipeline, MAGeCK-iNC (MAGeCK including Negative Controls, available at kampmannlab.ucsf.edu/mageck-inc). This pipeline integrates a published method, MAGeCK (Li et al., 2014) with aspects of our previous bioinformatics pipeline (Kampmann et al., 2013, 2014) to take full advantage of the non-targeting control sgRNAs in our library when computing P values (see Methods for details). Based on the depletion or enrichment of sgRNAs targeting specific genes, we identified hit genes for which knockdown was toxic or beneficial to either iPSCs or neurons at different time points (Fig. 2B and Supplemental Fig. S2B). We then calculated a knockdown phenotype score and significance P value for each gene (Supplemental Table S1). Knockdown phenotypes of hit genes were strongly correlated between neurons at different time points, but distinctly less correlated between neurons and iPSCs (Fig. 2C). Next, we compared genes that were essential in iPSCs and/or neurons in our screens with "gold-standard" essential genes that were previously identified through genetic screens in cancer cell lines (Hart et al., 2014). This analysis revealed a shared core set of essential genes, as expected, and additional iPSC-specific and neuron-specific essential genes (Fig. 2D).

Using Gene Set Enrichment Analysis (GSEA) (Mootha et al., 2003; Subramanian et al., 2005), we found enrichment of distinct groups of survival-related genes in neurons compared to iPSCs, such as genes associated with steroid metabolism (Supplemental Fig. S2C). We determined expression levels of genes at different time points during neuronal differentiation by Quant-Seq (Data deposited in GEO, GSE124703; the results can be visualized at kampmannlab.ucsf.edu/ineuron-rna-seq). As a group, neuron-essential genes were expressed at significantly higher levels than non-essential genes in iPSC-derived neurons (one-sided Mann-Whitney U test, Supplemental Fig. S2D). The vast majority of neuron-essential genes were detectable at the transcript level, further supporting the specificity of our screen results.

Intriguingly, we identified several genes that specifically enhanced neuronal survival when knocked down, including *MAP3K12* (encoding dual leucine zipper kinase DLK), *MAPK8* (encoding Jun kinase JNK1), *CDKN1C* (encoding the cyclin-dependent kinase inhibitor p57) and *EIF2AK3* (encoding the eIF2alpha kinase PERK) (Supplemental Table S1). A pathway involving DLK, JNK and PERK has previously been implicated in neuronal death (Ghosh et al., 2011; Huntwork-Rodriguez et al., 2013; Larhammar et al., 2017; Miller et al., 2009; Pozniak et al., 2013; Watkins et al., 2013; Welsbie et al., 2013), validating our approach.

In summary, our large-scale CRISPRi screen in human iPSC-derived neurons uncovered genes that controlled the survival of neurons, but not cancer cells or iPSCs, demonstrating the potential of our platform to characterize the biology of differentiated cell types.

Pooled validation of hit genes

To validate and further characterize hit genes from the primary large-scale screen, we performed a series of secondary screens. For this purpose, we generated a new lentiviral sgRNA plasmid (pMK1334) that enables screens with single-cell RNA-Seq (scRNA-Seq) readouts (based on the

CROP-Seq format (Datlinger et al., 2017)), and high-content imaging readouts (expressing a bright, nuclear-targeted BFP) (Fig. 3A). We individually cloned 192 sgRNAs into this plasmid (184 sgRNAs targeting 92 different hit genes with two sgRNAs per gene and eight non-targeting control sgRNAs). Then, to confirm essential genes identified in our primary screen, we pooled these plasmids and conducted a survival-based validation screen (Fig. 3A). Because the library size was small compared to the primary screen, we obtained a high representation of each sgRNA in the validation screen. As in the primary screen, CRISPRi-i^{3}N iPSCs transduced with the plasmid pool were either passaged as iPSCs or differentiated into glutamatergic neurons, and then harvested at different time points for next-generation sequencing and calculation of survival phenotypes for each sgRNA (Supplemental Table S2). We observed a high correlation of raw sgRNA counts between two biological replicates ($R^2 > 0.9$, Fig. 3B), supporting the robustness of phenotypes measured in the pooled validation screen. We then compared the results from the validation screen results with those from the primary screen. In both iPSCs and neurons, all positive hits and most of the negative hits from the primary screen were confirmed in the validation screen (Fig. 3C). These findings indicate that hits identified in the primary screen are highly reproducible.

In the brain, many neuronal functions are supported by glial cells, particularly astrocytes. To rule out the possibility that hits from the primary screen were artifacts of an astrocyte-free culture environment, we included an additional condition in the validation screen, in which neurons were co-cultured with primary mouse astrocytes. We found that neuronal phenotypes in the presence or absence of astrocytes were highly correlated (Fig. 3D,E and Supplemental Fig. S3A), indicating that the vast majority of the neuron-essential genes we identified are required even in the presence of astrocytes. However, we identified a small number of genes, including *PPCDC*, *UROD* and *MAT2A*, for which knockdown was less toxic in the presence of astrocytes (Fig. 3F). This suggests that astrocytes may compensate for the cell-autonomous loss of function for these genes in neurons. We also identified a small number of other genes, including *MMAB*, *UBA1* and *PPP2R2A*, for which knockdown was more toxic in the presence of astrocytes (Fig. 3F). These genes may function in pathways affected by crosstalk between neurons and astrocytes.

Inducible CRISPRi distinguishes neuronal differentiation and survival phenotypes

A caveat of our primary screen is that we introduced the sgRNA library into cells constitutively expressing CRISPRi machinery at the iPSC stage. Therefore, some hit genes detected in the primary screen may play a role in neuronal differentiation rather than neuronal survival. To explore this possibility, we developed a system to allow us to independently control neuronal differentiation and CRISPRi activity. We generated inducible CRISPRi constructs by tagging the CRISPRi machinery (dCas9-BFP-KRAB) with dihydrofolate reductase (DHFR) degron. In the absence of the small molecule trimethoprim (TMP), these DHFR degrons cause proteasomal degradation of fused proteins. Addition of TMP counteracts degradation (Iwamoto et al., 2010). Our initial construct contained a single N-terminal DHFR degron (Supplemental Fig. S3B), which was insufficient to fully suppress CRISPRi activity in the absence of TMP (Supplemental Fig. S3C). Therefore, we generated another plasmid (pRT029) with DHFR degrons on both the N- and C- termini of dCas9-BFP-KRAB (Figure 3G). This dual-degron CRISPRi construct was then integrated into the CLYBL locus of i^{3}N-iPSCs. In the absence of TMP, the double-degron construct had no CRISPRi activity in iPSCs or neurons (Supplemental Fig. S3D). TMP addition starting at the iPSC stage resulted in robust CRISPRi activity in iPSCs and neurons

(Supplemental Fig. S3D), and addition TMP addition starting at the neuronal stage resulted in moderate CRISPRi activity (Supplemental Fig. S3E). While future optimization of the inducible CRISPRi construct will be necessary, these results indicate that temporal regulation of CRISPRi activity can be achieved in iPSCs and differentiated neurons.

We used the inducible CRISPRi platform to determine if hit genes from our primary screen were related to neuronal survival or differentiation. iPSCs expressing the dual-degron construct were transduced with the pooled validation sgRNA library. Cells were then cultured under three different conditions, including no TMP (-/- TMP), TMP added starting at the iPSC stage (+/+ TMP), and TMP added at the neuronal stage (-/+ TMP) (Figure 3H). In the population cultured without TMP, none of the sgRNAs showed strong phenotypes compared to cells to which TMP was added at the iPSC stage (Figure 3I), confirming the tight control of the inducible system. To determine if any of the neuron-essential genes identified in our primary screen were in actuality required for differentiation, we compared neurons in which knockdown was induced either at the iPSC stage or later at the neuronal stage of the protocol. Phenotypes observed in these two conditions were highly correlated ($r = 0.98$, Fig. 3J), indicating that the vast majority of hits identified from the original screen are indeed essential for neuronal survival, rather than differentiation (Fig. 3H).

Interestingly, there was one exception: sgRNAs targeting *PPP1R12C* were strongly enriched when TMP was added at the iPSC stage, but this phenotype was substantially weaker when TMP was added at the neuron stage. Since the AAVS1 locus resides within the *PPP1R12C* gene, we speculated that sgRNAs targeting *PPP1R12C* interfered with neuronal differentiation driven by doxycycline-mediated induction of Ngn2 from the AAVS1-integrated expression cassette. Indeed, we observed that two independent sgRNAs targeting *PPP1R12C* each caused continued proliferation instead of neuronal differentiation in a subset of iPSCs (Supplemental Fig. S3F,G), providing a possible explanation for the enrichment of cells expressing *PPP1R12C*-targeted sgRNAs in the primary screen. Thus, our inducible CRISPRi approach successfully uncovered a false-positive hit from the primary screen caused by a technical artifact.

Taken together, these pooled validation screens confirmed that hits from the primary screen were highly reproducible and that we were able to identify genes specifically essential for neuronal survival.

CROP-Seq generates mechanistic hypotheses for genes controlling neuronal survival

Recently developed strategies to couple CRISPR screening to single-cell RNA-Seq readouts yield rich, high-dimensional phenotypes from pooled screens (Adamson et al., 2016; Datlinger et al., 2017; Dixit et al., 2016). As a first step towards understanding the mechanisms by which hit genes affect the survival of iPSCs and neurons, we investigated how gene knockdown altered transcriptomes of single cells (Fig. 4A) using a modified version of the CROP-Seq approach (Datlinger et al., 2017). We selected 27 genes that exemplified different categories of hits based on their pattern of survival phenotypes in iPSCs and neurons (Fig. 3E). A pool of 58 sgRNAs (two sgRNAs targeting each selected gene and 4 non-targeting control sgRNAs) in the secondary screening plasmid pMK1334 (Fig. 3A) was transduced into CRISPRi-i^{3}N iPSCs. We used the 10x Genomics platform to perform single-cell RNA sequencing (scRNA-Seq) of ~ 20,000 iPSCs and 20,000 Day 7 neurons. Transcripts containing sgRNA sequences were further amplified to facilitate sgRNA identity assignment, adapting a previously published strategy (Hill et al., 2018). Following sequencing, transcriptomes and sgRNA identities were mapped to individual cells (Data deposited in GEO, GSE124703; see Methods). High data quality was evident from the

mean reads per cell (~84,000 for iPSCs, ~91,000 for neurons), the median number of genes detected per cell (~5,000 for iPSCs, ~4,600 for neurons) and the number of cells to which a unique sgRNA could be assigned after quality control (~15,000 iPSCs, ~8,400 neurons).

Next, we examined the transcriptomes of groups of cells expressing a given sgRNA (which we refer to as "sgRNA groups"). In both iPSCs and neurons, the two sgRNA groups expressing sgRNAs targeting the same gene tended to form clusters in t-Distributed stochastic neighbor embedding (tSNE) plots (Supplemental Fig. S4A), confirming that independent sgRNAs targeting the same gene had highly similar phenotypic consequences. The extent of gene knockdown varied across cells within an sgRNA group and between the two sgRNAs targeting the gene. To characterize phenotypes in cells with the most stringent gene knockdown, we took advantage of the single-cell resolution of the CROP-Seq data to select the top 50% of cells with the best on-target knockdown for each gene for further analysis. We refer to this group of cells as the "gene knockdown group". Compared to cells with non-targeting sgRNAs, the expression levels of the targeted genes in a gene knockdown group were greatly repressed (Supplemental Fig. S4B). For most genes (24/27 in iPSCs and 18/27 in neurons) knockdown levels of greater than 80% were achieved. Together, these findings further support the robustness of CRISPRi knockdown and of the transcriptomic phenotypes determined by our modified CROPseq platform.

To characterize how gene knockdown altered transcriptomes of iPSCs and neurons, we performed differential expression analysis between gene knockdown groups and the negative control group (Supplemental Table S3). By clustering gene knockdown groups based on the signature of differential gene expression, we found transcriptomic signatures associated with knockdown of functionally related genes (Fig. 4B). For some genes, knockdown resulted in upregulation of functionally related genes. For example, knockdown of genes involved in cholesterol and fatty acid biosynthesis, including *HMGCS1*, *HMGCR*, *PMVK*, *MVK*, *MMAB*, and *HACD2*, caused induction of other genes in the same pathway (Fig. 4B and Supplemental Table S3). Thus, pooled CROP-Seq screens can identify and group functionally related genes in human neurons.

The CROP-Seq screen also generated mechanistic hypotheses for how knockdown of individual genes controls neuronal survival. For example, knockdown of *MAP3K12* specifically improved neuronal survival. Signaling by the *MAP3K12*-encoded kinase DLK had previously been implicated in neuronal death and neurodegeneration (Ghosh et al., 2011; Huntwork-Rodriguez et al., 2013; Larhammar et al., 2017; Miller et al., 2009; Pozniak et al., 2013; Watkins et al., 2013; Welsbie et al., 2013). In our screen, knockdown of *MAP3K12* resulted in pervasive, coherent changes in neuronal gene expression (Fig. 4C and Supplemental Table S4). Ribosomal genes and the anti-apoptotic transcription factor Brn3a (encoded by *POU4F1*) were upregulated. Conversely, we observed downregulation of the pro-apoptotic BCL-2 protein Harakiri/DP5 (encoded by *HRK*), the neurodegeneration-associated amyloid precursor protein (*APP*), and the pro-apoptotic transcription factor *JUN*, which is also a downstream signaling target of DLK in the context of neuronal death (Welsbie et al., 2013). Furthermore, *MAP3K12* knockdown caused downregulation of a vast array of proteins involved in cytoskeletal organization and upregulation of specific synaptotagmins, which act as calcium sensors in synaptic vesicles. These changes in gene expression may relate to the function of DLK in synaptic terminals and its reported role as a neuronal sensor of cytoskeletal damage (Valakh et al., 2015). Lastly, *MAP3K12* knockdown induced expression of neuritin (*NRN1*), a neurotrophic factor associated with synaptic plasticity and neuritogenesis in model organisms (Cantallops et al., 2000; Javaherian and Cline, 2005;

Naeve et al., 1997; Yao et al., 2016). Intriguingly, neuritin levels are decreased in Alzheimer's Disease patient brains, and overexpression of neuritin was found to be protective in a mouse model of Alzheimer's Disease (Choi et al., 2014). Thus, CROP-Seq provides a wealth of testable hypotheses for neuroprotective mechanisms and specific effectors downstream of DLK/*MAP3K12* inhibition.

CROP-Seq reveals neuron-specific transcriptomic consequences of gene knockdown

The results from our parallel CROP-Seq screens in iPSCs and neurons enabled us to compare transcriptomic consequences of gene knockdown across both cell types (Supplemental Fig. S5A). Interestingly, only a few genes, including *SQLE*, *MMAB*, *MVK*, *UQCRQ*, and *ATP5B*, showed high similarity (similarity score > 0.15) in the transcriptomic changes they induced in iPSCs versus neurons. Knockdown of most genes induced distinct transcriptomic responses in these two cell types. This suggests that either gene knockdown caused different stress states in the two cell types or that gene regulatory networks are wired differently in iPSC and iPSC-derived neurons.

To further dissect these cell type-specific phenotypes, we ranked genes by the similarity of their knockdown phenotypes in iPSCs and neurons with respect to survival and transcriptomic response (Fig. 5A). For some genes, both survival and transcriptomic phenotypes were similar in iPSCs and neurons. An example for this category of genes is *UQCRQ*, which encodes a component of the mitochondrial complex III in the electron transport chain. *UQCRQ* is essential in both cell types, and knockdown of *UQCRQ* had similar transcriptomic consequences in both iPSCs and neurons – upregulation of mitochondrially encoded electron transport chain components and of ribosomal proteins (Supplemental Fig. S5B). Similarly, knockdown of cholesterol and fatty acid biosynthesis genes induced expression of other cholesterol and fatty acid biosynthesis genes in both iPSCs and neurons (Fig. 4B and Supplemental Table S3).

Interestingly, we also found examples of genes that were essential in both neurons and iPSCs yet caused substantially different transcriptomic phenotypes when knocked down. For example, knockdown of the essential E1 ubiquitin activating enzyme, *UBA1*, caused neuron-specific induction of a large number of genes (Supplemental Fig. S5C), including those encoding heat shock proteins (cytosolic chaperones *HSPA8* and *HSPB1* and endoplasmic reticulum chaperones *HSPA5* and *HSP90B1*). This suggests that compromised *UBA1* function triggered a broad proteotoxic stress response in neurons, but not iPSCs, consistent with the role of *UBA1* in several neurodegenerative diseases (Groen and Gillingwater, 2015). Thus, even ubiquitously expressed housekeeping genes can play distinct roles in different cell types.

Lastly, we discovered that some genes differed with respect to both survival and transcriptomic phenotypes in neurons and iPSCs. This was expected for genes predominantly expressed in neurons, such as *MAP3K12* (Fig. 4C). However, we also found examples of genes in which knockdown had strikingly different transcriptomic consequences in neurons and iPSCs despite high expression in both cell types. Such a gene is *MAT2A*, encoding methionine adenosyl transferase 2a, which catalyzes the production of the methyl donor S-adenosylmethionine (SAM) from methionine and ATP (Fig. 5B). *MAT2A* is essential in neurons, but not iPSCs (Fig. 5C). Knockdown of *MAT2A* in iPSCs did not substantially affect the expression of any gene other than *MAT2A* itself (Fig. 5D). In neurons, however, knockdown of *MAT2A* caused differential expression of thousands of genes (Fig. 5E and Supplemental Table S4). We used GSEA to investigate which genes were differentially expressed, and found that genes that were downregulated in neurons in response to *MAT2A* knockdown were enriched for neuron-specific

functions (Fig. 5F). This provides a possible explanation for the neuron-selective toxicity of *MAT2A* knockdown.

In summary, results from CROP-Seq screens in iPSCs and iPSC-derived neurons further highlight differences in gene function across different two cell types, provide rich insights into consequences of gene knockdown, and generate mechanistic hypotheses. They further support the idea that it is critically important to study gene function in relevant cell types, even for widely expressed genes.

An arrayed CRISPRi platform for rich phenotyping by longitudinal imaging

While pooled genetic screens are extremely powerful due to their scalability, many cellular phenotypes that cannot be evaluated using a pooled approach. Such phenotypes include cellular morphology, temporal dynamics, electrophysiological properties, and non-cell-autonomous phenotypes. To expand the utility of our screening platform, we therefore optimized an arrayed CRISPRi platform for iPSC-derived neurons.

As a proof-of-concept arrayed screen, we established a longitudinal imaging platform to track the effect of knocking down selected hit genes from our primary screen on neuronal survival and morphology over time. First, we stably expressed cytosolic mScarlet (for neurite tracing) and nuclear-localized mNeon-Green (for survival analysis) in CRISPRi-i^{3}N iPSCs. Then, we infected these iPSCs in multi-well plates with lentivirus encoding individual sgRNAs, followed by puromycin selection and neuronal differentiation. After three days, we re-plated pre-differentiated neurons on 96-well plates alongside similarly prepared cells that did not express sgRNAs or the cytosolic mScarlet marker at a 1:20 ratio. This co-culture approach allowed more accurate neuronal tracing of mScarlet-expressing neurons. These plates were then longitudinally imaged every few days using an automated microscope with a large area of each well imaged at each time point, allowing us to re-image the same populations of neurons over time (Fig. 6A and Supplemental Movies S1 and S2).

We developed an automated image analysis pipeline to segment neuronal cell bodies and neurites (Fig. 6B). By tracking cell numbers over time, we could measure neuronal survival and iPSC proliferation (Fig. 6C,D). Quantification of survival based on longitudinal imaging was robust across biological replicates (Supplemental Fig. S6). As anticipated, the vast majority of sgRNAs that altered neuronal and iPSC survival in pooled screens also altered survival in our arrayed longitudinal survival analysis. Cell type-specific survival effects were also recapitulated in the arrayed screen format (Fig. 6D). However, longitudinal imaging provided additional information on the timeline of toxicity caused by knockdown of different genes and revealed gene-specific temporal patterns (Fig. 6D,E). These experiments showed that arrayed CRISPRi survival screens in iPSC-derived neurons are possible, and complement data generated from pooled screens.

We then analyzed the effect of gene knockdown on neurite morphology. Our neurite segmentation algorithm extracted multiple quantitative metrics related to neuronal morphology, including neurite length, number of neurite trunks and neurite branching (Fig. 6B,C). Surprisingly, knockdown of different genes that we previously implicated in neuronal survival also had distinct effects on neuronal morphology (Fig. 6C,F). Additionally, we found that neurite length and the number of neurite trunks were under independent genetic control (Fig. 6G). Taken together, the profile of features extracted from our imaging platform was so information-rich and gene-specific that hierarchical clustering of individual sgRNAs based on these features led to co-clustering of the two sgRNAs targeting a given gene for the majority of genes (Fig. 6E).

Conceptually, knockdown phenotypes of specific genes occupy distinct regions in a high-dimensional neuronal morphology space (Fig. 6E,G). In combination with survival-based and CROP-Seq screen, our multimodal CRISPRi platform will enable the deep characterization of gene function in a plethora of human cell types.

DISCUSSION

Here, we describe a platform for large-scale, multimodal CRISPRi-based genetic screens in human iPSC-derived neurons. While CRISPR screens in cancer cells and stem cells have revealed numerous biological insights, we reasoned that screens in differentiated, non-cancerous cell types could elucidate novel, cell-type specific gene functions. Indeed, our survival screens uncovered genes that were essential for neurons, but not iPSCs or cancer cells. We also found that knockdown of some broadly-expressed housekeeping genes, such as *UBA1*, caused strikingly-distinct transcriptomic phenotypes in neurons compared to iPSCs, consistent with the idea that gene functions can vary across distinct cell types. Lastly, our arrayed screening platform uncovered gene-specific effects on longitudinal survival and neuronal morphology. These proof-of-concept screens have generated a wealth of phenotypic data, which will provide a rich resource for further analysis and the generation of mechanistic hypotheses.

The combination of CRISPRi functional genomics and iPSC-derived neuron technology leverages the strengths of both approaches. Neurons are a highly specialized and disease-relevant cell type, and thus it is crucial to study certain human gene functions in these cells. However, primary human neurons cannot readily be obtained in the quantities and homogeneity needed for large-scale screens. By contrast, human iPSCs have several fundamental qualities ideally suited for screens. They can be made from readily available cells, such as skin fibroblasts or peripheral mononuclear blood cells; they can be genetically engineered and subsequently expanded to generate large numbers of isogenic cells; and they can then be differentiated into a variety of cell types, including specific neuronal subtypes. Differentiation protocols based on induced expression of transcription factors are particularly useful for screens, as they are rapid and yield large numbers of homogeneous neurons. In addition to the Ngn2-driven generation of cortical glutamatergic neurons (Fernandopulle et al., 2018; Wang et al., 2017; Zhang et al., 2013) used here, induced expression of different transcription factors yield other types of neurons, such as motor neurons (Hester et al., 2011; Shi et al., 2018) and inhibitory neurons (Yang et al., 2017). Systematic screens are beginning to uncover additional combinations of transcription factors driving specific neuronal fates (Liu et al., 2018; Tsunemoto et al., 2018). Thus, iPSC technology could be used to generate different neuron types from an isogenic parental cell line, which would facilitate parallel CRISPR screens to dissect neuronal subtype specific gene function. Such screens will address fundamental questions in neuroscience, such as why specific neuronal subtypes are selectively vulnerable in neurodegenerative diseases (Kampmann, 2017). Furthermore, genetic modifier screens in neurons derived from patient iPSCs and isogenic controls have the potential to uncover new disease mechanisms. These discoveries may, in turn, yield new therapeutic strategies to correct cellular defects linked to disease genes. Despite their usefulness, iPSC-derived neurons have limitations – in particular, they do not fully recapitulate all features of mature (or aging) neurons in the human brain. We anticipate that functional genomics approaches, such as ours, may hold the key to improving protocols that lead to ever more faithful models of mature human neurons.

CRISPRi is particularly well suited as a method to study gene function in iPSC-derived neurons, for several reasons. First, it does cause DNA damage, and thus lacks the non-specific p53-mediated toxicity observed with CRISPRn approaches in iPSCs and untransformed cells (Haapaniemi et al., 2018; Ihry et al., 2018). Second, it is inducible and reversible (Gilbert et al., 2014), enabling the time-resolved dissection of human gene function. Third, it perturbs gene function via partial knockdown, as opposed to knockout, thereby enabling functional characterization of essential genes, as demonstrated in this study.

There are several areas for further development of our platform. Further optimization of inducible CRISPRi will result in more potent gene repression in mature neurons, leading to increased sensitivity. Also, establishment of our CRISPR activation (CRISPRa) approach in iPSC-derived neurons will enable gain-of-function genetic screens, which yield complementary insights to CRISPRi loss-of-function screens (Gilbert et al., 2014). Finally, using synthetic sgRNAs instead of lentivirus in arrayed CRISPRi screens would substantially increase scalability.

We anticipate that the technology described here can be broadly applied to include additional neuron-relevant readouts, such as multi-electrode arrays (to measure electrophysiological properties) and brain organoids (to assay interactions of neurons with other cell types). However, our technology is not limited to neurons, and should provide a paradigm for investigating the specific biology of numerous other types of differentiated cells. Systematic parallel genetic screens across the full gamut of human cell types cells may uncover context-specific roles of human genes, leading to a deeper mechanistic understanding of how they control human biology and disease.

ACKNOWLEDGEMENTS

We thank Li Gan, Bruce Conklin, Forbes D. Porter, and Christopher Wassif for support and advice, Kun Leng for sharing unpublished constructs, Andrew Hill for advice on CROP-Seq, Kun Leng, Emmy Li and Rene Sit for advice on scRNA-Seq, Sami Barmada for advice on longitudinal neuron survival analysis, Nina Dräger for gift of primary astrocytes, Eric Chow and Derek Bogdanoff for next-generation sequencing, Avi Samelson for comments on this manuscript, and members of the Kampmann and Ward Labs for discussions.

This research was supported by the Intramural Research Program of the NIH/NINDS, an NIH Director's New Innovator Award (NIH/NIGMS DP2 GM119139 to M.K.), NIH/NIA grants (R01 AG062359 and R56 AG057528 to M.K.), the NINDS Tau Center Without Walls (NIH/NINDS U54 NS100717 to M.K.), an Allen Distinguished Investigator Award to M.K. (Paul G. Allen Family Foundation, to M.K.), a Chan-Zuckerberg Biohub Investigator Award (to M.K.), and a Tau Consortium Investigator Award (Rainwater Charitable Foundation, to M.K.).

AUTHOR CONTRIBUTIONS

R.T., M.A.G., C.H.L., M.E.W. and M.K. contributed to the study's overall conception, design and interpretation, and wrote the manuscript and created the Figures with input from the other authors. R.T. designed and conducted the validation screens and CROP-Seq screens and designed and conducted computational analyses for all screens (including survival screens, CROP-Seq, and longitudinal imaging screens), with guidance from M.K. M.A.G. designed and conducted imaging screens with guidance from M.E.W. and M.K. C.H.L. established CRISPRi in iPSC-derived neurons and designed and conducted the primary screens with guidance from R.T. and M.K. C.H.L. also conducted and analyzed Quant-Seq experiments and created the

iNeuronRNASeq web application. M.A.G., M.T.L., M.S.F., and R.P. designed, generated and characterized constructs and cell lines, with guidance from M.E.W. and M.K. J.Y.H. and D.N. generated and characterized constructs and cell lines, with guidance from R.T. and M.K. A.V.P. contributed to validation experiments.

DECLARATIONS OF INTEREST

M.K. has filed a patent application related to CRISPRi and CRISPRa screening (PCT/US15/40449).

REFERENCES

Adamson, B., Norman, T.M., Jost, M., Cho, M.Y., Nunez, J.K., Chen, Y., Villalta, J.E., Gilbert, L.A., Horlbeck, M.A., Hein, M.Y., *et al.* (2016). A Multiplexed Single-Cell CRISPR Screening Platform Enables Systematic Dissection of the Unfolded Protein Response. Cell *167*, 1867-1882 e1821.

Cantallops, I., Haas, K., and Cline, H.T. (2000). Postsynaptic CPG15 promotes synaptic maturation and presynaptic axon arbor elaboration in vivo. Nature neuroscience *3*, 1004-1011.

Cerbini, T., Funahashi, R., Luo, Y., Liu, C., Park, K., Rao, M., Malik, N., and Zou, J. (2015). Transcription activator-like effector nuclease (TALEN)-mediated CLYBL targeting enables enhanced transgene expression and one-step generation of dual reporter human induced pluripotent stem cell (iPSC) and neural stem cell (NSC) lines. PloS one *10*, e0116032.

Choi, Y., Lee, K., Ryu, J., Kim, H.G., Jeong, A.Y., Woo, R.S., Lee, J.H., Hyun, J.W., Hahn, S., Kim, J.H., *et al.* (2014). Neuritin attenuates cognitive function impairments in tg2576 mouse model of Alzheimer's disease. PloS one *9*, e104121.

Datlinger, P., Rendeiro, A.F., Schmidl, C., Krausgruber, T., Traxler, P., Klughammer, J., Schuster, L.C., Kuchler, A., Alpar, D., and Bock, C. (2017). Pooled CRISPR screening with single-cell transcriptome readout. Nat Methods *14*, 297-301.

Dixit, A., Parnas, O., Li, B., Chen, J., Fulco, C.P., Jerby-Arnon, L., Marjanovic, N.D., Dionne, D., Burks, T., Raychowdhury, R., *et al.* (2016). Perturb-Seq: Dissecting Molecular Circuits with Scalable Single-Cell RNA Profiling of Pooled Genetic Screens. Cell *167*, 1853-1866 e1817.

Fernandopulle, M.S., Prestil, R., Grunseich, C., Wang, C., Gan, L., and Ward, M.E. (2018). Transcription Factor-Mediated Differentiation of Human iPSCs into Neurons. Curr Protoc Cell Biol *79*, e51.

Ghosh, A.S., Wang, B., Pozniak, C.D., Chen, M., Watts, R.J., and Lewcock, J.W. (2011). DLK induces developmental neuronal degeneration via selective regulation of proapoptotic JNK activity. J Cell Biol *194*, 751-764.

Gilbert, L.A., Horlbeck, M.A., Adamson, B., Villalta, J.E., Chen, Y., Whitehead, E.H., Guimaraes, C., Panning, B., Ploegh, H.L., Bassik, M.C., *et al.* (2014). Genome-Scale CRISPR-Mediated Control of Gene Repression and Activation. Cell *159*, 647-661.

Gilbert, L.A., Larson, M.H., Morsut, L., Liu, Z., Brar, G.A., Torres, S.E., Stern-Ginossar, N., Brandman, O., Whitehead, E.H., Doudna, J.A., *et al.* (2013). CRISPR-mediated modular RNA-guided regulation of transcription in eukaryotes. Cell *154*, 442-451.

Groen, E.J.N., and Gillingwater, T.H. (2015). UBA1: At the Crossroads of Ubiquitin Homeostasis and Neurodegeneration. Trends in molecular medicine *21*, 622-632.

Haapaniemi, E., Botla, S., Persson, J., Schmierer, B., and Taipale, J. (2018). CRISPR–Cas9 genome editing induces a p53-mediated DNA damage response. Nature medicine *24*, 927-930.

Hart, T., Brown, K.R., Sircoulomb, F., Rottapel, R., and Moffat, J. (2014). Measuring error rates in genomic perturbation screens: gold standards for human functional genomics. Mol Syst Biol *10*, 733.

Hester, M.E., Murtha, M.J., Song, S., Rao, M., Miranda, C.J., Meyer, K., Tian, J., Boulting, G., Shaffer, D.V., Zhu, M.X., *et al.* (2011). Rapid and Efficient Generation of Functional Motor Neurons From Human Pluripotent Stem Cells Using Gene Delivered Transcription Factor Codes. Molecular Therapy *19*, 1905-1912.

Hill, A.J., McFaline-Figueroa, J.L., Starita, L.M., Gasperini, M.J., Matreyek, K.A., Packer, J., Jackson, D., Shendure, J., and Trapnell, C. (2018). On the design of CRISPR-based single-cell molecular screens. Nat Methods *15*, 271-274.

Horlbeck, M.A., Gilbert, L.A., Villalta, J.E., Adamson, B., Pak, R.A., Chen, Y., Fields, A.P., Park, C.Y., Corn, J.E., Kampmann, M., *et al.* (2016). Compact and highly active next-generation libraries for CRISPR-mediated gene repression and activation. eLife *5*.

Huntwork-Rodriguez, S., Wang, B., Watkins, T., Ghosh, A.S., Pozniak, C.D., Bustos, D., Newton, K., Kirkpatrick, D.S., and Lewcock, J.W. (2013). JNK-mediated phosphorylation of DLK suppresses its ubiquitination to promote neuronal apoptosis. J Cell Biol *202*, 747-763.

Ihry, R.J., Worringer, K.A., Salick, M.R., Frias, E., Ho, D., Theriault, K., Kommineni, S., Chen, J., Sondey, M., Ye, C., *et al.* (2018). p53 inhibits CRISPR-Cas9 engineering in human pluripotent stem cells. Nature medicine *24*, 939-946.

Iwamoto, M., Bjorklund, T., Lundberg, C., Kirik, D., and Wandless, T.J. (2010). A general chemical method to regulate protein stability in the mammalian central nervous system. Chemistry & biology *17*, 981-988.

Javaherian, A., and Cline, H.T. (2005). Coordinated motor neuron axon growth and neuromuscular synaptogenesis are promoted by CPG15 in vivo. Neuron *45*, 505-512.

Kampmann, M. (2017). A CRISPR Approach to Neurodegenerative Diseases. Trends in molecular medicine *23*, 483-485.

Kampmann, M. (2018). CRISPRi and CRISPRa Screens in Mammalian Cells for Precision Biology and Medicine. ACS Chem Biol *13*, 406-416.

Kampmann, M., Bassik, M.C., and Weissman, J.S. (2013). Integrated platform for genome-wide screening and construction of high-density genetic interaction maps in mammalian cells. Proceedings of the National Academy of Sciences of the United States of America *110*, E2317-2326.

Kampmann, M., Bassik, M.C., and Weissman, J.S. (2014). Functional genomics platform for pooled screening and generation of mammalian genetic interaction maps. Nature protocols *9*, 1825-1847.

Koike-Yusa, H., Li, Y., Tan, E.P., Velasco-Herrera Mdel, C., and Yusa, K. (2014). Genome-wide recessive genetic screening in mammalian cells with a lentiviral CRISPR-guide RNA library. Nat Biotechnol *32*, 267-273.

Langmead, B., Trapnell, C., Pop, M., and Salzberg, S.L. (2009). Ultrafast and memory-efficient alignment of short DNA sequences to the human genome. Genome biology *10*, R25.

Larhammar, M., Huntwork-Rodriguez, S., Jiang, Z., Solanoy, H., Sengupta Ghosh, A., Wang, B., Kaminker, J.S., Huang, K., Eastham-Anderson, J., Siu, M., *et al.* (2017). Dual leucine zipper kinase-dependent PERK activation contributes to neuronal degeneration following insult. eLife *6*.

Li, W., Xu, H., Xiao, T., Cong, L., Love, M.I., Zhang, F., Irizarry, R.A., Liu, J.S., Brown, M., and Liu, X.S. (2014). MAGeCK enables robust identification of essential genes from genome-scale CRISPR/Cas9 knockout screens. Genome biology *15*, 554.

Liu, Y., Yu, C., Daley, T.P., Wang, F., Cao, W.S., Bhate, S., Lin, X., Still, C., Liu, H., Zhao, D., *et al.* (2018). CRISPR Activation Screens Systematically Identify Factors that Drive Neuronal Fate and Reprogramming. Cell Stem Cell *23*, 758-771.

Mandegar, M.A., Huebsch, N., Frolov, E.B., Shin, E., Truong, A., Olvera, M.P., Chan, A.H., Miyaoka, Y., Holmes, K., Spencer, C.I., *et al.* (2016). CRISPR Interference Efficiently Induces Specific and Reversible Gene Silencing in Human iPSCs. Cell Stem Cell *18*, 541-553.

McCarthy, D.J., Campbell, K.R., Lun, A.T., and Wills, Q.F. (2017). Scater: pre-processing, quality control, normalization and visualization of single-cell RNA-seq data in R. Bioinformatics *33*, 1179-1186.

Miller, B.R., Press, C., Daniels, R.W., Sasaki, Y., Milbrandt, J., and DiAntonio, A. (2009). A dual leucine kinase-dependent axon self-destruction program promotes Wallerian degeneration. Nature neuroscience *12*, 387-389.

Mootha, V.K., Lindgren, C.M., Eriksson, K.F., Subramanian, A., Sihag, S., Lehar, J., Puigserver, P., Carlsson, E., Ridderstrale, M., Laurila, E., *et al.* (2003). PGC-1alpha-responsive genes involved in oxidative phosphorylation are coordinately downregulated in human diabetes. Nature genetics *34*, 267-273.

Naeve, G.S., Ramakrishnan, M., Kramer, R., Hevroni, D., Citri, Y., and Theill, L.E. (1997). Neuritin: a gene induced by neural activity and neurotrophins that promotes neuritogenesis.

Proceedings of the National Academy of Sciences of the United States of America *94*, 2648-2653.

Pozniak, C.D., Sengupta Ghosh, A., Gogineni, A., Hanson, J.E., Lee, S.H., Larson, J.L., Solanoy, H., Bustos, D., Li, H., Ngu, H., *et al.* (2013). Dual leucine zipper kinase is required for excitotoxicity-induced neuronal degeneration. J Exp Med *210*, 2553-2567.

Robinson, M.D., McCarthy, D.J., and Smyth, G.K. (2010). edgeR: a Bioconductor package for differential expression analysis of digital gene expression data. Bioinformatics *26*, 139-140.

Rosenbluh, J., Xu, H., Harrington, W., Gill, S., Wang, X., Vazquez, F., Root, D.E., Tsherniak, A., and Hahn, W.C. (2017). Complementary information derived from CRISPR Cas9 mediated gene deletion and suppression. Nat Commun *8*, 15403.

Sergushichev, A. (2016). An algorithm for fast preranked gene set enrichment analysis using cumulative statistic calculation. bioRxiv *doi:* https://doi.org/10.1101/060012.

Shalem, O., Sanjana, N.E., Hartenian, E., Shi, X., Scott, D.A., Mikkelsen, T.S., Heckl, D., Ebert, B.L., Root, D.E., Doench, J.G., *et al.* (2014). Genome-scale CRISPR-Cas9 knockout screening in human cells. Science *343*, 84-87.

Shi, Y., Lin, S., Staats, K.A., Li, Y., Chang, W.-H., Hung, S.-T., Hendricks, E., Linares, G.R., Wang, Y., Son, E.Y., *et al.* (2018). Haploinsufficiency leads to neurodegeneration in C9ORF72 ALS/FTD human induced motor neurons. Nature medicine *24*, 313-325.

Smith, A., Ramos-Morales, F., Ashworth, A., and Collins, M. (1997). A role for JNK/SAPK in proliferation, but not apoptosis, of IL-3-dependent cells. Current Biology *7*, 893-896.

Subramanian, A., Tamayo, P., Mootha, V.K., Mukherjee, S., Ebert, B.L., Gillette, M.A., Paulovich, A., Pomeroy, S.L., Golub, T.R., Lander, E.S., *et al.* (2005). Gene set enrichment analysis: a knowledge-based approach for interpreting genome-wide expression profiles. Proceedings of the National Academy of Sciences of the United States of America *102*, 15545-15550.

Tsunemoto, R., Lee, S., Szücs, A., Chubukov, P., Sokolova, I., Blanchard, J.W., Eade, K.T., Bruggemann, J., Wu, C., Torkamani, A., *et al.* (2018). Diverse reprogramming codes for neuronal identity. Nature *557*, 375-380.

Valakh, V., Frey, E., Babetto, E., Walker, L.J., and DiAntonio, A. (2015). Cytoskeletal disruption activates the DLK/JNK pathway, which promotes axonal regeneration and mimics a preconditioning injury. Neurobiol Dis *77*, 13-25.

Wang, C., Ward, M.E., Chen, R., Liu, K., Tracy, T.E., Chen, X., Xie, M., Sohn, P.D., Ludwig, C., Meyer-Franke, A., *et al.* (2017). Scalable Production of iPSC-Derived Human Neurons to Identify Tau-Lowering Compounds by High-Content Screening. Stem cell reports *9*, 1221-1233.

Wang, T., Wei, J.J., Sabatini, D.M., and Lander, E.S. (2014). Genetic screens in human cells using the CRISPR-Cas9 system. Science *343*, 80-84.

Watkins, T.A., Wang, B., Huntwork-Rodriguez, S., Yang, J., Jiang, Z., Eastham-Anderson, J., Modrusan, Z., Kaminker, J.S., Tessier-Lavigne, M., and Lewcock, J.W. (2013). DLK initiates a transcriptional program that couples apoptotic and regenerative responses to axonal injury. Proceedings of the National Academy of Sciences of the United States of America *110*, 4039-4044.

Welsbie, D.S., Yang, Z., Ge, Y., Mitchell, K.L., Zhou, X., Martin, S.E., Berlinicke, C.A., Hackler, L., Jr., Fuller, J., Fu, J., *et al.* (2013). Functional genomic screening identifies dual leucine zipper kinase as a key mediator of retinal ganglion cell death. Proceedings of the National Academy of Sciences of the United States of America *110*, 4045-4050.

Willsey, A.J., Morris, M.T., Wang, S., Willsey, H.R., Sun, N., Teerikorpi, N., Baum, T.B., Cagney, G., Bender, K.J., Desai, T.A., *et al.* (2018). The Psychiatric Cell Map Initiative: A Convergent Systems Biological Approach to Illuminating Key Molecular Pathways in Neuropsychiatric Disorders. Cell *174*, 505-520.

Yang, N., Chanda, S., Marro, S., Ng, Y., Janas, J.A., Haag, D., Ang, C.E., Tang, Y., Flores, Q., Mall, M., *et al.* (2017). Generation of pure GABAergic neurons by transcription factor programming. Nature Methods *14*, 621-628.

Yao, J.J., Zhao, Q.R., Liu, D.D., Chow, C.W., and Mei, Y.A. (2016). Neuritin Up-regulates Kv4.2 alpha-Subunit of Potassium Channel Expression and Affects Neuronal Excitability by Regulating the Calcium-Calcineurin-NFATc4 Signaling Pathway. The Journal of biological chemistry *291*, 17369-17381.

Zhang, B., Kirov, S., and Snoddy, J. (2005). WebGestalt: an integrated system for exploring gene sets in various biological contexts. Nucleic acids research *33*.

Zhang, Y., Pak, C., Han, Y., Ahlenius, H., Zhang, Z., Chanda, S., Marro, S., Patzke, C., Acuna, C., Covy, J., *et al.* (2013). Rapid Single-Step Induction of Functional Neurons from Human Pluripotent Stem Cells. Neuron *78*, 785-798.

Zhou, Y., Zhu, S., Cai, C., Yuan, P., Li, C., Huang, Y., and Wei, W. (2014). High-throughput screening of a CRISPR/Cas9 library for functional genomics in human cells. Nature *509*, 487-491.

FIGURE TITLES AND LEGENDS

Fig. 1. Durable gene knockdown by CRISPR interference in human iPSC-derived neurons.

(**A**) Construct pC13N-dCas9-BFP-KRAB for the expression of CRISPRi machinery from the CLYBL safe-harbor locus: catalytically dead Cas9 (dCas9) fused to blue fluorescent protein (BFP) and the KRAB domain, under the control of the constitutive CAG promoter.

(**B**) Knockdown of the transferrin receptor (*TFRC*) in iPSC-derived neurons. iPSCs expressing the CRISPRi machinery were lentivirally infected with an sgRNA targeting *TFRC* or a non-targeting negative control sgRNA. Neuronal differentiation was induced by addition of doxycycline on Day -3 of the differentiation protocol and plating cells in neuronal medium on Day 0. Cells were harvested at different days, and levels of *TFRC* and *GAPDH* mRNAs were quantified by qPCR. After normalizing each sample by *GAPDH* mRNA levels, ratios of *TFRC* mRNA were calculated for cells expressing the *TFRC*-targeting sgRNA versus the non-targeting sgRNA. Mean and standard deviations for replicates are shown.

(**C**) Knockdown of progranulin (*GRN*) in iPSC-derived neurons monitored at the protein level by immunofluorescence (IF) microscopy. *Top row*, non-targeting negative control sgRNA. *Bottom row*, sgRNA targeting progranulin. For cells infected with progranulin-targeting sgRNA, progranulin signal (IF, green) is substantially reduced compared with cells infected with non-targeting sgRNA. Neuronal marker Tuj1 (IF, red) and nuclear counterstain DRAQ5 (blue) are shown.

Fig. 2. Massively parallel screen for essential genes in iPSCs and iPSC-derived neurons

(A) Strategy for pooled screen for essential genes. iPSCs constitutively expressing the CRISPRi machinery were transduced with a lentiviral library of 13,025 sgRNAs targeting 2,325 genes encoding kinases and other proteins representing the druggable genome (Horlbeck et al., 2016). Following transduction, cells were passaged as iPSCs or differentiated into glutamatergic neurons. Samples of cell populations were taken at different time points, and frequencies of cells expressing a given sgRNA were determined by next-generation sequencing of the sgRNA-encoding locus in genomic DNA isolated from the cell populations.

(B) Volcano plots summarizing knockdown phenotypes and statistical significance (Mann-Whitney U test) for genes targeted in the pooled screen. *Top*, phenotypes for proliferation/survival of iPSCs between Day 0 and Day 10. *Bottom*, phenotypes for survival of iPSC-derived neurons between Day 0 and Day 28. Dashed lines represent the cutoff for hit genes, which was defined based on the product of phenotype and $-\log_{10}$(P value) at an empirically determined false discovery rate of 0.05 (see Methods). All screen results are provided as Supplemental Table S1.

(C) Correlation of hit gene strength (the product of phenotype and $-\log_{10}$(P value)) obtained for Day 10 iPSCs, and neurons harvested on Day 14, 21, or 28 post-induction.

(D) Overlap between essential genes we identified here in iPSCs and neurons, as well as between gold-standard essential genes defined previously for cancer cell lines (Hart et al., 2014).

Figure 3. Pooled validation of hit genes from the primary screen

(A) Strategy for validation of hit genes. 192 sgRNAs were individually cloned into the secondary screening vector pMK1334, including 184 sgRNAs targeting 92 hit genes (two sgRNAs per gene) and 8 non-targeting control sgRNAs. CRISPRi-i^{3}N iPSCs were transduced with a pool of these plasmids and passaged as iPSCs or differentiated into glutamatergic neurons. Differentiated neurons were either in monocultures or co-cultured with primary mouse astrocytes. Samples of the cell populations were taken at different time points, and frequencies of cells expressing a given sgRNA were determined by next-generation sequencing as in the primary screen. Each cell population had two biological replicates.

(B) Raw counts of sgRNAs from next-generation sequencing are shown for biological replicates of Day 10 iPSCs (left) and Day 14 neurons (right). Each dot represents one sgRNA. Coefficients of determination (R^2) were calculated.

(C) Knockdown phenotype scores from primary screens and validation screens are shown for Day 10 iPSCs (left) and Day 14 neurons (right). Each dot represents one gene. Pearson correlation coefficients (r) were calculated.

(D) Hierarchical clustering of different cell populations from the pooled validation screens based on the pairwise correlations of the knockdown phenotype scores of all genes.

(E) Heatmap showing knockdown phenotype scores of the genes targeted in the validation screen (columns) in different cell populations (rows). Both genes and cell populations were hierarchically clustered based on Pearson correlation. Red asterisks mark genes selected for secondary screens (CROP-Seq and longitudinal imaging). All results from the pooled validation screens are provided in Supplemental Table S2.

(F) Scatter plot showing gene knockdown phenotype scores of Day 14 neurons in monoculture (x-axis) and co-culture with primary mouse astrocytes (y-axis). Each dot represents one gene. Outlier genes, whose differences of knockdown phenotype scores between mono-culture and co-culture were greater than ± 2 standard deviations away from the mean differences of all genes, are labeled. The Pearson correlation coefficient (r) is shown.

(G) Strategy for degron-based inducible CRISPRi. *Top*, construct pRT029 for the expression of CRISPRi machinery (dCas9-BFP-KRAB) fused to two DHFR degrons from the CLYBL safe-harbor locus. *Bottom*, degron-tagged CRISPRi machinery is degraded in the absence of the DHFR degron stabilizer trimethoprim (TMP). Addition of TMP stabilizes the degron-tagged construct, inducing CRISPRi activity.

(H) Strategy to test whether hit genes control neuronal survival or earlier processes. The pooled validation sgRNA library is introduced into inducible CRISPRi iPSCs. Cells are cultured under three different conditions: no TMP (-/- TMP), TMP added from the iPSC stage (+/+ TMP), and

TMP added from the neuronal stage (-/+ TMP). Each screen is conducted in duplicate. Phenotypes are determined by next-generation sequencing as in the previous validation screens.

(I) Knockdown phenotype scores for Day 14 neurons from screens in the inducible CRISPRi iPSCs, comparing populations with TMP added from the iPSC stage (x-axis) to populations without TMP added (y-axis). Each dot represents one gene.

(J) Knockdown phenotype scores for Day 14 neurons from screens in the inducible CRISPRi iPSCs, comparing populations with TMP added from the iPSC stage (x-axis) to populations with TMP added from the neuronal stage (y-axis). Each dot represents one gene. The outlier gene, *PPP1R12C,* is labeled. The Pearson correlation coefficient (r) is shown.

Figure 4. CROP-Seq reveals transcriptome changes in iPSCs and iPSC-derived neurons induced by knockdown of survival-relevant genes

(**A**) Strategy for CROP-Seq experiments. iPSCs expressing constitutive CRISPRi were transduced with a pool of CROP-Seq sgRNAs containing 54 sgRNAs targeting 27 selected essential genes (2 sgRNAs/gene) and 4 non-targeting control sgRNAs. Following transduction, cells were passaged as iPSCs or differentiated into glutamatergic neurons. Single-cell transcriptomes and sgRNA identities were obtained by scRNA-Seq. sgRNA transcripts were additionally amplified to improve sgRNA identity assignment.

(**B**) Heatmaps showing changes in gene expression in response to CRISPRi knockdown of genes of interest in iPSCs (top) and Day 7 neurons (bottom). Each row represents the targeted gene for one gene knockdown group. For each gene knockdown group, the top 20 genes with the most significantly altered expression level relative to the negative control group were selected, and the merged set of these genes is represented by the columns. Rows and columns were clustered hierarchically based on Pearson correlation. Functionally related groups of differentially expressed genes are labeled. The underlying dataset is provided as Supplemental Table S3.

(**C**) MA plot showing changes in transcript levels caused by *MAP3K12* knockdown in iPSC-derived neurons, which were obtained from the CROP-Seq screen. Differentially expressed genes (padj < 0.05) were colored red (upregulation) or blue (downregulation), and selected genes and gene groups are labeled and discussed in the main text.

Figure 5. Cell-type specific responses to gene knockdown on the transcriptomic level.

(**A**) Comparison of differences between iPSCs and neurons in knockdown phenotypes for survival and transcriptomic responses. Genes were ranked by similarities between iPSCs and neurons in their knockdown phenotypes in terms of survival (x-axis) or transcriptomic response (y-axis). Dashed lines indicate the middle rank positions. Genes selected for further discussion are labeled in red.

(B) Methionine adenosyl transferase 2a (*MAT2A*) was selected for further analysis. MAT2A catalyzes the production of the methyl donor S-adenosylmethionine (SAM) from methionine and ATP.

(**C**) *MAT2A* is essential in neurons but not iPSCs. Knockdown phenotypes of *MAT2A* in iPSCs and iPSC-derived neurons from the primary and validation screens. Survival phenotypes of 2 sgRNAs targeting *MAT2A* were averaged and error bars represent standard deviation.

(**D,E**) MA plots showing changes in transcript levels caused by *MAT2A* knockdown in (D) iPSCs and (E) iPSC-derived neurons. Gene expression profiles of *MAT2A* knockdown were obtained from CROP-Seq and were compared to negative controls. Differentially expressed genes (padj < 0.05) were colored red (upregulation) or blue (downregulation). The dot representing *MAT2A* is labeled.

(**F**) Gene Set Enrichment Analysis (GSEA) results for differentially expressed genes in iPSC-derived neurons with *MAT2A* knockdown compared to negative control neurons. Significantly enriched GO terms for Biological Process (left) and Cellular Component (right) are shown.

Figure 6. Longitudinal imaging to track the effect of selected hit gene knockdown on iPSC growth, neuronal survival and neurite morphology

(A) Strategy for longitudinal imaging for neuronal survival and neurite morphology**.** CRISPRi-i^{3}N iPSCs expressing cytosolic mScarlet and nuclear mNeonGreen were infected with individual sgRNAs targeting selected hit genes. Infected cells were selected by puromycin. Following three days of pre-differentiation, 5% of these cells, alongside 95% of similarly prepared cells that did not express cytosolic mScarlet marker nor were exposed to lentivirus containing sgRNAs, were plated in wells of 96-well plates. These plates were then imaged at different days of differentiation and the images were analyzed using an automated image analysis pipeline to quantify neuronal survival and neurite morphology.

(B) An example illustrating the image analysis pipeline. A raw image (left) containing sgRNA positive neurons expressing nuclear BFP (shown in cyan) and cytosolic mScarlet (shown in greyscale) were segmented and neurites were recognized (right). Different parameters, including neurite length, number of neurite trunks and number of neurite branches were quantified for individual neurons. Total number of sgRNA positive neurons was quantified for each image to monitor neuronal survival.

(C) Quantification of knockdown effects of *PGGT1B* and *PPP2R1A* on neuronal survival, neurite length, number of branches and number of trunks. For each sgRNA, mean ± SD of replicate images is shown for each time point. *** represents significant differences compared to non-targeting sgRNA ($P < 0.001$, Student's t-test).

(D) Examples of hit genes whose survival phenotypes in the pooled screens were validated by longitudinal imaging. *Top*, knockdown phenotypes of *SQLE*, *HMGCR*, *MAT2A* and *MAP3K12* in iPSCs and iPSC-derived neurons from the validation screens. Survival phenotypes of two

sgRNAs targeting each gene were averaged and error bars represent standard deviation. *Middle and bottom*, growth curves of iPSCs (middle) and survival curves of neurons (bottom) with non-targeting sgRNAs and sgRNAs targeting *SQLE, HMGCR, MAT2A* or *MAP3K12*. Fold change (for iPSCs, middle) or surviving fraction (for neurons, bottom) of number of sgRNA positive cells relative to Day 1 was calculated for each imaging well and all replicate wells for one sgRNA were averaged. Error bars represent standard deviation.

(E) Heatmap showing percentage changes of neuronal survival and neurite morphology features relative to non-targeting sgRNAs at different time points (columns) induced by knockdown of different genes (rows). Rows were hierarchically clustered based on Pearson correlation.

(F) Representative images of neurons with *PGGT1B* and *PPP2R1A* knockdown on Days 1, 5 and 10. Nuclear BFP is shown in blue, cytosolic mScarlet is shown in red. Scale bar, 100 μm.

(G) Scatter plot showing the effect of gene knockdown on neurite length (x-axis) and number of neurite trunks (y-axis). Each dot indicates the mean measurements of all neurons in one image. Different target genes are shown in different colors, and replicate images for one target gene are grouped by dashed lines in the same colors.

METHODS

Generation of DNA constructs

The CLYBL-targeting constitutive CRISPRi vector pC13N-dCas9-BFP-KRAB was obtained by sub-cloning dCas9-BFP-KRAB from plasmid pHR-SFFV-dCas9-BFP-KRAB downstream of a CAG promoter in the CLYBL-targeting pC13N-iCAG.copGFP vector via BsrGI and AgeI digestion, thus replacing copGFP and generating the plasmid. pHR-SFFV-dCas9-BFP-KRAB was a gift from Stanley Qi & Jonathan Weissman, Addgene plasmid # 46911; http://n2t.net/addgene:46911 ; RRID:Addgene_46911 (Gilbert et al., 2013) and pC13N-iCAG.copGFP was a gift from Jizhong Zou (Addgene plasmid # 66578 ; http://n2t.net/addgene:66578 ; RRID:Addgene_66578 (Cerbini et al., 2015)).

The AAVS1-targeting constitutive CRISPRi vector pMTL3 was obtained by inserting a gene block (gBlock, IDT Technologies) encoding BFP-KRAB into pAAVS1-NC-CRISPRi to create a C-terminal fusion with dCas9, and replacing the neomycin resistance marker with a puromycin resistance marker. pAAVS1-NC-CRISPRi (Gen3) was a gift from Bruce Conklin (Addgene plasmid # 73499 ; http://n2t.net/addgene:73499 ; RRID:Addgene_73499 (Mandegar et al., 2016)). The degron controlled version was generated by inserting a gene-block encoding *E. coli* dihydrofolate reductase (ecDHFR)–derived degrons with the R12Y, G67S, and Y100I mutations (Iwamoto et al., 2010) to generate an N-terminal fusion with the CRISPRi machinery.

The CLYBL-targeted inducible CRISPRi construct pRT029 was generated by sub-cloning gene blocks encoding *E. coli* dihydrofolate reductase (ecDHFR)–derived degrons with the R12Y, G67S, and Y100I mutations in the first degron and R12H, N18T and A19V in the second degron (Iwamoto et al., 2010) to generate both an N-terminal and a C-terminal in-frame fusion with dCas9-BFP-KRAB in pC13N-dCas9-BFP-KRAB.

The secondary screening vector pMK1334 was generated as follows: The PpuMI – SnaBI fragment of CROPseq-Guide-Puro was replaced with a gene block encoding the mU6-BstXI-BlpI-optimized sgRNA backbone fragment from our sgRNA vector pCRISPRia-v2 (Addgene plasmid # 84832 ; http://n2t.net/addgene:84832 ; RRID:Addgene_84832 (Horlbeck et al., 2016)) to obtain pMK1332. CROPseq-Guide-Puro was a gift from Christoph Bock (Addgene plasmid # 86708 ; http://n2t.net/addgene:86708 ; RRID:Addgene_86708 (Datlinger et al., 2017)). Next, the RsrII + PflMI fragment from pMK1332 was replaced by the RsrII + PflMI fragment from pCRISPRia-v2 to introduce tagBFP, creating pMK1333. Last, tagBFP was replaced by a gene block encoding 2xmycNLS-tagBFP2 to obtain pMK1334.

The mNeon-Green-NLS vector (H53) was generated by sub-cloning an EF1α promoter and mNeon-Green with two SV40-NLS into the pMK1333 vector via XhoI and EcoRI digestion, thus replacing the mU6 promoter, the original EF1α promoter, and the original fluorophore. The mScarlet vector (I2) was generated by sub-cloning mScarlet downstream of an EF1α promoter in the H53 vector via BmtI and EcoRI digestion, thus replacing mNeon-Green-NLS.

Vector maps are available at kampmannlab.ucsf.edu/resources, and plasmids will be shared on Addgene.

Human iPS cell culture

Human iPSCs (WTC11 background) were cultured in Essential 8 Medium (Gibco/Thermo Fisher Scientific; Cat. No. A1517001) on BioLite Cell Culture Treated Dishes (Thermo Fisher Scientific; assorted Cat. No.) coated with Growth Factor Reduced, Phenol Red-Free, LDEV-Free Matrigel Basement Membrane Matrix (Corning; Cat. No. 356231) diluted 1:100 in Knockout

DMEM (Gibco/Thermo Fisher Scientific; Cat. No. 10829-018). Briefly, Essential 8 Medium was replaced every other day or every day once 50% confluent. When 80-90% confluent, cells were passaged, which entailed the following: aspirating media, washing with DPBS, incubating with StemPro Accutase Cell Dissociation Reagent (Gibco/Thermo Fisher Scientific; Cat. No. A11105-01) at 37°C for 7 minutes, diluting Accutase 1:5 in DPBS, collecting in conicals, centrifuging at 200g for 5 minutes, aspirating supernatant, resuspending in Essential 8 Medium supplemented with 10nM Y-27632 dihydrochloride ROCK inhibitor (Tocris; Cat. No. 125410), counting, and plating onto Matrigel-coated plates at desired number.

CRISPRi iPS cell line generation

WTC11 iPSCs harboring a single-copy of doxycycline-inducible mouse NGN2 at the AAVS1 locus (Wang et al., 2017)(Fernandopulle et al., 2018) were used as the parental iPSC line for further genetic engineering. iPSCs were transfected with pC13N-dCas9-BFP-KRAB and TALENS targeting the human CLYBL intragenic safe harbor locus (between exons 2 and 3) (pZT-C13-R1 and pZT-C13-L1, Addgene #62196, #62197) using DNA In-Stem (VitaScientific). After 14 days, BFP-positive iPSCs were isolated via FACS sorting, and individualized cells were plated in a serial dilution series to enable isolation of individual clones under direct visualization with an inverted microscope (EtaLuma LS 620) in a tissue culture hood via manual scraping. Clones with heterozygous integration of dCas9-BFP-KRAB (determined using PCR genotyping) were used for further testing. Karyotype testing (Cell Line Genetics) was normal for the clonal line used for further experiments in this study, which we termed CRISPRi-i^{3}N iPSCs. Similarly, we generated the inducible CRISPRi iPSC line by using pRT029 as a donor plasmid, instead of pC13N-dCas9-BFP-KRAB.

Human neuronal culture

Human iPSCs engineered to express mNGN2 under a doxycycline-inducible system in the AAVS1 safe harbor locus were used for the differentiation protocol below. iPSCs were released and centrifuged as above, and pelleted cells were resuspended in N2 Pre-Differentiation Medium containing the following: Knockout DMEM/F12 (Gibco/Thermo Fisher Scientific; Cat. No. 12660-012) as the base, 1X MEM Non-Essential Amino Acids (Gibco/Thermo Fisher Scientific; Cat. No. 11140-050), 1X N2 Supplement (Gibco/Thermo Fisher Scientific; Cat. No. 17502-048), 10ng/mL NT-3 (PeproTech; Cat. No. 450-03), 10ng/mL BDNF (PeproTech; Cat. No. 450-02), 1μg/mL Mouse Laminin (Thermo Fisher Scientific; Cat. No. 23017-015), 10nM ROCK inhibitor, and 2μg/mL doxycycline hydrochloride (Sigma-Aldrich; Cat. No. D3447-500MG) to induce expression of mNGN2. iPSCs were counted and plated at 7 x 10^5 cells per Matrigel-coated well of a 6-well plate in 2mL of N2 Pre-Differentiation Medium, or at 4 x 10^6 cells per Matrigel-coated 10-cm dish in 12mL of medium, for three days. After three days, hereafter Day 0, pre-differentiated cells were released and centrifuged as above, and pelleted cells were resuspended in Classic Neuronal Medium containing the following: half DMEM/F12 (Gibco/Thermo Fisher Scientific; Cat. No. 11320-033) and half Neurobasal-A (Gibco/Thermo Fisher Scientific; Cat. No. 10888-022) as the base, 1X MEM Non-Essential Amino Acids, 0.5X GlutaMAX Supplement (Gibco/Thermo Fisher Scientific; Cat. No. 35050-061), 0.5X N2 Supplment, 0.5X B27 Supplement (Gibco/Thermo Fisher Scientific; Cat. No. 17504-044), 10ng/mL NT-3, 10ng/mL BDNF, 1μg/mL Mouse Laminin, and 2μg/mL doxycycline hydrochloride. Pre-differentiated cells were subsequently counted and plated plated at 2 x 10^5 cells per well of a BioCoat Poly-D-Lysine 12-well plate (Corning; Cat. No. 356470) in 1mL of

Classic Neuronal Medium, or at 7.5 x 10^6 cells per BioCoat Poly-D-Lysine 10-cm dish (Corning; Cat. No. 356469) in 10mL medium. On Day 7, half of the medium was removed and an equal volume of fresh Classic Neuronal Medium without doxycycline was added. On Day 14, half of the medium was removed and twice that volume of fresh medium without doxycycline was added. On Day 21, one-third of the medium was removed and twice that volume of fresh medium without doxycycline was added. On Day 28 and each week after, one-third of the medium was removed and an equal volume of fresh medium without doxycycline was added.

For the longitudinal imaging screens, updated media formulations were used for neuronal differentiation and culture. During the three days of pre-differentiation, we used Induction Medium containing the following: Knockout DMEM/F12 (Gibco/Thermo Fisher Scientific; Cat. No. 12660-012) as the base, 1X GlutaMAX Supplement (Gibco/Thermo Fisher Scientific; Cat. No. 35050-061), 1X MEM Non-Essential Amino Acids (Gibco/Thermo Fisher Scientific; Cat. No. 11140-050), 1X N2 Supplement (Gibco/Thermo Fisher Scientific; Cat. No. 17502-048), 10nM ROCK inhibitor, and 2ug/mL doxycycline (Sigma #D9891). Differentiated neurons were cultured in Cortical Neuron Culture Medium containing the following: BrainPhys Neuronal Medium (STEMCELL Technologies #05790) or BrainPhys without Phenol Red (STEMCELL Technologies #05791) as the base, 1X B27 Supplement (Gibco/Thermo Fisher Scientific; Cat. No. 17504-044), 10ng/mL NT-3 (PeproTech; Cat. No. 450-03), 10ng/mL BDNF (PeproTech; Cat. No. 450-02), 1ug/mL Mouse Laminin (R&D Systems #3446-005-01), and optionally 2μg/mL doxycycline.

Astrocyte co-culture

Primary mouse astrocytes were isolated from 2 P1 mouse pups and cultured in T75 in DMEM + 10% FBS. One day after plating neurons, astrocytes were dissociated by trypsin, washed by PBS to remove any remaining FBS and centrifuged at 200g for 5 minutes. The pelleted astrocytes were resuspended in the Classic Neuronal Medium and plated onto the neuronal culture at a 1:5 astrocytes to neurons ratio. Media changes were performed as indicated above for neuronal culture. Once astrocytes were confluent, 2 μM final concentration of AraC was added to the culture.

Releasing neurons with papain for downstream applications

Papain (Worthington; Code: PAP2; Cat. No.LK003178) was resuspended in 1X Hanks' Balanced Salt Solution (Corning; Cat. No. 21-022-CV) to 20U/mL and warmed at 37°C for 10 minutes. Magnesium chloride was added at 5mM and DNase (Worthington; Code: DPRF; Cat. No. LS006333) was added at 5ug/mL immediately before use. Culture medium was aspirated and human iPSC-derived neurons were washed with DPBS. The papain, magnesium chloride, and DNase solution was added at 250μL per well of a 12-well plate or at 2mL per 10-cm dish and incubated at 37°C for 10 minutes. This dissociation solution was quenched in 5 volumes of DMEM (Gibco/Thermo Fisher Scientific; Cat. No. 10313-039) supplemented with 10% fetal bovine serum for each volume of dissociation solution, and the resulting solution was used to detach and transfer the sheet of cells to the appropriate collection tube format. For DNA, RNA, or protein extraction, the neuron sheet was centrifuged at 200g for 3 minutes, the supernatant was carefully removed with a P1000 pipette, and the pellet was snap frozen in liquid nitrogen. For flow cytometry analysis, the neuron sheet was triturated 10-15 times and centrifuged at 200g for 10 minutes, the supernatant was carefully removed with a P1000 pipette, and the pellet was resuspended in staining solution.

Quantitative validation of CRISPRi activity by qPCR
Human iPSCs or neuron cell pellets were thawed on ice, and total RNA was extracted using the Quick-RNA Miniprep Kit (Zymo; Cat. No. R1054). An input of 100ng RNA was used to synthesize cDNA with the SuperScript III First-Strand Synthesis System (Invitrogen; Cat. No. 18080-051). Samples were prepared for qPCR in technical duplicates in 15µL reaction volumes using SensiFAST SYBR Lo-ROX 2X master mix (Bioline; Cat. No. BIO-94005), custom qPCR primers from Integrated DNA Technologies used at a final concentration of 0.4uM, and cDNA (prepared above) diluted at 1:2 or 1:100 for the target or housekeeping gene, respectively. Quantitative real-time PCR was performed on an Agilent Mx3005P QPCR System with the following Fast 2-Step protocol: 1) 95°C for 2 minutes; 2) 95°C for 5 seconds (denaturation); 3) 60°C for 15 seconds (annealing/extension); 4) repeat steps 2 and 3 for a total of 40 cycles; 5) ramp from 55°C to 95°C to establish melting curve. Expression fold changes were calculated using the ΔΔCt method.

Qualitative validation of CRISPRi activity by immunocytochemistry
Pre-differentiated neurons were plated in Classic Neuronal Medium with doxycycline on day 0 at 4×10^4 cells per well on sterilized, Matrigel-coated 12mm diameter round glass coverslips (Ted Pella Inc; Cat. No. 26023) placed in 24-well plates. One day later, primary rat cortical astrocytes (gift from Li Gan) were plated in Classic Neuronal Medium with doxycycline on the same coverslips (co-culture) at 8×10^3 cells per well. On days 7 and 14, half of the medium was removed and an equal volume of fresh Classic Neuronal Medium without doxycycline was added. On day 18, culture medium was aspirated from each well and cells were subsequently washed with DPBS. Cells were then fixed with 4% paraformaldehyde, which was prepared by diluting 16% paraformaldehyde (Electron Microscopy Sciences; Cat. No. 15710) 1:4 in DPBS, at room temperature for 15 minutes. Paraformaldehyde was removed with a P1000 pipette and collected for proper disposal, and coverslips were washed three times with DPBS for 5 minutes each. Cells were blocked with 2.5ug/mL Mouse BD Fc Block (BD Biosciences; Cat. No. 553141) at room temperature for 15 minutes and subsequently incubated with 1uL mouse IgG1k anti-human CD325 antibody conjugated to APC (BioLegend; Cat. No. 350808) in 50uL of Fc Block at room temperature for 45 minutes. Coverslips were then washed once with DPBS for 5 minutes, incubated with 1ug/mL Hoechst 33342 (Thermo Fisher Scientific; Cat. No. H3570) diluted in DPBS at room temperature for 10 minutes, and then washed twice more with DPBS for 5 minutes each. One drop of Aqua Poly Mount (Polysciences; Cat. No. 18606)

Pre-differentiated neurons were plated in Cortical Neuron Culture Medium with doxycycline on Day 0 at 3.0×10^5 cells per well on poly-L-ornithine-coated 8-well glass-bottom slides (Ibidi #80827). On day 5, culture medium was aspirated from each well and cells were subsequently washed with PBS. Cells were fixed with 4% paraformaldehyde, which was prepared by diluting 16% paraformaldehyde (Electron Microscopy Sciences; Cat. No. 15710) 1:4 in PBS, at room temperature for 30 minutes. Paraformaldehyde was removed with a P1000 pipette and collected for proper disposal, and slides were washed three times with PBS. Cells were blocked with 3% donkey serum with 0.1% saponin in PBS at room temperature for one hour and subsequently incubated with goat anti-human progranulin antibody diluted 1:3000 (R&D Systems #AF2420) and mouse anti-human TUJ1 antibody (BioLegend #801201) diluted 1:1000 in blocking buffer at 4°C overnight. Slides were then washed three times with PBS and incubated with donkey anti-goat IgG conjugated to AF-488 (Jackson ImmunoResearch #705-

545-147) and donkey anti-mouse IgG conjugated to RRX (Jackson ImmunoResearch #715-295-151) diluted 1:2000 in blocking buffer at room temperature for one hour. Slides were again washed three times with PBS, and incubated with 5 uM DRAQ5 (Thermo Fisher Scientific #62251) in blocking buffer at room temperature for 30 minutes.

Primary screen

The CRISPRi v2 H1 library with top 5 sgRNAs per gene (Horlbeck et al., 2016) was packaged into lentivirus for transduction of iPSCs as follows. Two 15-cm dishes were each seeded with 8 x 10^6 HEK293T cells in 20 mL DMEM complete (basal medium supplemented with 10% FBS and 1% penicillin/streptomycin). The next day, H1 library transfection mix was prepared in the following manner: 10ug H1 library plasmid and 10ug third generation packaging mix (1:1:1 mix of the three plasmids) were diluted into 2mL Opti-MEM I Reduced Serum Medium (Gibco; Cat. No. 31985070); 250uL Lipofectamine 2000 Transfection Reagent (Invitrogen; Cat. No. 11668027) was diluted into 2mL Opti-MEM and incubated at room temperature for 5 minutes; the diluted DNA solution was added to the diluted Lipofectamine solution, inverted several times to mix, and incubated at room temperature for 15 minutes. Following incubation, half of the transfection solution was gently added dropwise to each 15-cm dish with HEK293T cells, and the plates were briefly and gently moved in a figure-eight pattern to mix. Eight hours later, the Lipofectamine-containing media on each dish was carefully aspirated and replaced with 20mL DMEM complete supplemented with 40uL ViralBoost (Alstem; Cat. No. VB100; diluted 1:500 in media). Two days later, HEK293T media (approximately 40mL) was transferred to a 50mL conical and centrifuged at room temperature for 10 minutes at 300g to pellet cell debris. The supernatant was carefully transferred to a syringe fitted with a 0.45um filter in order to filter the virus-containing solution into a new 50mL conical. Approximately 10mL of cold Lentivirus Precipitation Solution (Alstem; Cat. No. VC100) was added to this filtered solution, which was then mixed well and stored at 4°C for 48 hours. Following incubation, the solution was centrifuged at 4°C for 30 minutes at 1,500g, and the supernatant was decanted. A second centrifugation at 4°C for 5 minutes at 1,500g was performed, and the remaining supernatant was removed with a P1000 pipette. The virus-containing pellet was resuspended in 20mL Essential 8 iPSC medium with ROCK inhibitor.

For infection with the H1 library, two T175 Matrigel-coated flasks were each seeded with 2 x 10^7 CRISPRi-i^3N iPSCs in 10mL of the virus-containing medium and left in the tissue culture hood for 15 minutes to allow even distribution and attachment before moving to the incubator. Six hours later, an additional 15mL of Essential 8 medium with ROCK inhibitor was added to each flask without removing the virus-containing medium. The next day, we performed a complete media change on all flasks, adding 35mL Essential 8 medium with ROCK inhibitor to allow the cells to recover and proliferate. One day later, we released the cells and seeded four T175 Matrigel-coated flasks each with 1 x 10^7 cells in 20mL Essential 8 medium with ROCK inhibitor, which was the medium volume and formulation used for puromycin treatment to enrich sgRNA-expressing cells. Treatment proceeded in the following manner: two days with 0.8ug/mL puromycin, followed by two days with 1ug/mL puromycin. At the end of treatment, cells were assessed by flow cytometry (83% expressed high levels of BFP) and seeded for the iPSC and neuronal survival screens, which are described below.

For the iPSC growth-based screen, two T175 Matrigel-coated flasks were each seeded with 1 x 10^7 cells in 20mL Essential 8 medium with ROCK inhibitor (timepoint t_0). Approximately 2 x 10^7 t_0 cells were also snap frozen in liquid nitrogen for downstream sample

preparation. Media was replaced on day two (t_2), omitting ROCK inhibitor. Cells were released on day three (t_3), and each replicate was seeded into two new T175 Matrigel-coated flasks with 1 x 10^7 cells each in 20mL Essential 8 medium with ROCK inhibitor. Media was replaced on day five (t_5), omitting ROCK inhibitor. Cells were released on day six (t_6), cells within the same replicate were mixed across flasks, and each replicate was seeded into two new T175 Matrigel-coated flasks with 1 x 10^7 cells each in 20mL Essential 8 medium with ROCK inhibitor. Media was replaced on days eight (t_8) and nine (t_9), omitting ROCK inhibitor. Cells were released on day ten (t_{10}), cells within the same replicate were mixed across flasks, and 4 x 10^7 cells from each replicate were snap frozen for downstream sample preparation.

For the neuronal survival screen, twelve 10-cm Matrigel-coated dishes were each seeded with 4 x 10^6 iPSCs in N2 Pre-Differentiation Medium (day -3) and differentiated as previously described. However, an additional full media change (10mL) was performed on Day 4 to remove cellular debris that started to appear. On Days 14, 21, and 28, dead (floating) and live (adherent) cells from two 10-cm dishes were harvested per replicate per timepoint. To collect dead cells, the media was harvested and centrifuged at room temperature for 10 minutes at 300g. The supernatant was decanted, and the pelleted cells were snap frozen for downstream sample preparation. To collect live cells, adherent cells were released by papain as previously described, and pelleted cells were snap frozen for downstream sample preparation. Genomic DNA was extracted with the NucleoSpin Blood L or XL kits (Macherey Nagel; Cat. No. 740954.20 or 740950.10, respectively) and samples were prepared for sequencing on an Illumina HiSeq-4000 based on previously described protocols (Gilbert et al., 2014; Kampmann et al., 2014).

Pooled validation screen

192 sgRNAs, including 184 sgRNAs targeting 92 selected hit genes from the primary screen (two sgRNAs per gene) and 8 non-targeting control sgRNAs, were individually cloned into the secondary screening vector pMK1334 and verified by Sanger sequencing. The plasmid was pooled and lentivirus was produced as for the Primary Screen. CRISPRi-i^3N iPSCs were transduced with the pool at a low multiplicity of infection and were selected by 1 ug/ml of puromycin. Following 3 days of expansion, approximately 2 million of these cells were harvested as Day 0 sample and the rest of cells were cultured as iPSCs (as described in 'Human iPS cell culture') or differentiated into glutamatergic neurons (as described in 'Human neuronal culture'). For the iPSC growth screen, iPSCs were cultured in E8 medium with daily medium change in 2 * T25 flasks as duplicates and were passaged every 2-3 days till Day 10. Approximately 2 million of Day 10 iPSCs from each replicate were harvested. For the mono-culture neuronal screen, 10 million of pre-differentiated neurons were plated in one Poly-D-Lysine coated 15-cm dish (Corning; Cat. No. 354550). Two replicate dishes of neurons were cultured in Classic Neuronal Medium as described in 'Human neuronal culture'. Day 14 and Day 28 neurons were harvested. For the co-culture neuronal screen, 1.5 million of primary mouse astrocytes were added into one Poly-D-Lysine coated 15-cm dish containing 7.5 million neurons. Two replicate dishes of neurons in co-culture were cultured as described in 'Astrocyte co-culture'. Day 14 neurons from each replicate of co-culture experiment were harvested. Genomic DNA was isolated from all harvested samples using a commercial kit (Macherey Nagel; NucleoSpin® Blood). The sgRNA-encoding region were then amplified and sequenced as in the Primary Screen.

CROP-Seq

CRISPRi-i^{3}N iPSCs were infected with a pool of selected sgRNAs in the CROP-Seq vector pMK1334 at a low multiplicity of infection to minimize double infection. After puromycin selection and expansion, cells were either passaged as iPSCs or differentiated into neurons. Approximately 20,000 iPSCs and 20,000 day 7 i^{3}Neurons were captured by the 10X Chromium Controller using Chromium Single Cell 3' Library & Gel Bead Kit v2 (10X Genomics; Cat. No. 120267) with 10,000 input cells per lane. Sample prep was performed according to protocol, holding 10-30 ng full-length cDNA for sgRNA-enrichment PCR.

To facilitate sgRNA assignment, sgRNA-containing transcripts were additionally amplified by hemi-nested PCR reactions by adapting a previously published approach (Hill et al., 2018). Briefly, in the first PCR reaction, 15ng of full-length cDNA was used as template and Enrichemnt_PCR_1_For and Enrichemnt_PCR_1_Rev were used as primers. PCR product was cleaned up by 1.0x SPRI beads (SPRIselect; BECKMAN COULTER; Cat. No. B23317) and 1ng cleaned product was input into the second PCR reaction using Enrichemnt_PCR_2_For and Enrichemnt_PCR_2_Rev as primers. Following 1.0x SPRI beads clean up, 1 ng of the PCR product from the second PCR reaction was used as template in the final PCR, in which reverse primer Enrichemnt_PCR_2_Rev and a forward primer, Enrichemnt_PCR_3_For, containing an i7 index, were used as primers. All PCR reactions were carried out for 18 cycles using KAPA HiFi polymerase (KAPA HiFi HotStart ReadyMix (2X); Cat. No. KK2602) with annealing temperature at 62 degree and 15 seconds extension per cycle. The sgRNA-enrichment libraries were separately indexed and sequenced as spike-ins alongside the whole-transcriptome scRNA-Seq libraries using NovaSeq 6000 using the following configuration:

Read 1: 26, i7 index: 8, i5 index: 0, Read 2: 98

Quant-Seq

Neurons cultured in 12-well plates were released with papain, pelleted, and snap frozen on days 0, 14, 21, 28, and 35 in technical duplicates (approximately 2 x 10^5 cells each) per timepoint. RNA was extracted using the Quick-RNA Miniprep Kit (Zymo; Cat. No. R1054), and RNA concentrations were determined with the Qubit RNA HS Assay Kit (Invitrogen; Cat. No. Q32855) on a Qubit 2.0 Fluorometer (Invitrogen; Cat. No. Q32866). mRNA-Seq libraries were prepared from an input of 184ng total RNA in 5uL using the QuantSeq 3' mRNA-Seq Library Prep Kit FWD for Illumina (Lexogen; Cat. No. 015). Briefly, oligodT hybridization enabled mRNA-selective reverse transcription. The original RNA template was then degraded, and second strand cDNA synthesis was achieved by random priming and extension by DNA polymerase. Samples were subsequently subjected to magnetic bead-based purification, followed by library amplification with indexed flow-cell adapters (14 PCR cycles) and another round of magnetic bead-based purification. mRNA-Seq library concentrations (mean of 1.01 ± 0.275 ng/uL) were measured with the Qubit dsDNA HS Assay Kit (Invitrogen; Cat. No. Q32851) on a Qubit 2.0 Fluorometer. Library fragment-length distributions (mean of 371 ± 16.1 bp) were quantified with the High Sensitivity DNA Kit (Agilent; Cat. No. 5067-4626) on a 2100 Bioanalyzer Instrument (Agilent; Cat. No. G2939BA). Molar concentrations for each sample were approximated from Qubit concentration (ng/uL) and mean fragment-length (bp) measurements using the following formula:

$$Molar\ Concentration = \frac{(Qubit\ Concentration)(1{,}000{,}000\ uL/L)}{\left(660\frac{ng}{nmol * bp}\right)(Mean\ Fragment\ Length)}$$

All libraries were diluted to 2.72nM for equimolar representation in the final, pooled sample. Single-end sequencing was performed, generating reads toward the poly(A) tail.

Longitudinal CRISPRi-i^{3}Neuron imaging

CRISPRi-i^{3}N iPSCs were transduced with lentivirus expressing mNeonGreen-NLS and FACS-sorted for the brightest green population. These polyclonal cells will be referred to as nuclear-green CRISPRi-i^{3}N iPSCs. Subsequently, a fraction of these iPSCs were transduced with lentivirus expressing cytosolic mScarlet and FACS sorted for the brightest red and green cells. These polyclonal iPSCs will be referred to as the nuclear-green/cytosolic red CRISPRi-i^{3}N iPSCs.

The arrayed sgRNAs in the pMK1334 vector were packaged into lentivirus for transduction of iPSCs as follows: 6-well plates coated with poly-D-lysine were seeded with 2.5 x 10^6 HEK293T cells per well in 1.5 mL of DMEM complete (basal medium supplemented with 10% FBS) each. The next day, the arrayed transfection mixes were prepared in the following manner: 1.2ug sgRNA plasmid and 1.2 ug packaging mix (0.8ug psPAX2, 0.3ug pMD2G, 0.1ug pAdVantage), along with 5 uL P3000 reagent (ThermoFisher Scientific # L3000015) were diluted into 150 uL Opti-MEM I Reduced Serum Medium (Gibco; Cat. No. 31985070); 3.75 uL Lipofectamine 3000 Transfection Reagent (ThermoFisher Scientific # L3000015) was diluted into 150 uL Opti-MEM and incubated at room temperature for 5 minutes; the diluted Lipofectamine solution was added to the diluted DNA solution, flicked to mix, and incubated at room temperature for 20 minutes. Following incubation, the transfection solutions were gently added dropwise to each well with HEK293T cells, and the plates were briefly and gently moved in a figure-eight pattern to mix. The following day, the Lipofectamine-containing media on each well was carefully aspirated and replaced with 3mL DMEM complete supplemented with 6uL ViralBoost (Alstem; Cat. No. VB100; diluted 1:500 in media). Three days later, HEK293T media from each well was transferred to one well each of two 2mL deep 96-well dishes (USA Scientific #1896-2800) and centrifuged at 4°C for 30 minutes at 3428g to pellet cell debris. Viral supernatant was stored at 4°C.

For functional titering of the lentivirus, nuclear-green+ CRISPRi-i^{3}N iPSCs were passaged and plated at a density of 1.0 x 10^4 cells/well in Matrigel-coated 96-well culture dishes. Following adherence of iPSCs, 75 uL of each viral supernatant was added to one well, and a series of half-volume dilutions was performed for a total of four dilutions. The following day, the culture medium containing the lentivrus was carefully aspirated and replaced with fresh medium. Three days after infection, iPSCs were imaged with a spinning disk confocal microscope with a motorized stage (Nikon Eclipse Ti), controlled using Nikon Elements software. A 20X objective was used to acquire a series of 36 slightly overlapping images within each well followed by image stitching. The ratio of cells infected with lentivirus was quantified via Nikon Elements software as the number of green nuclei with blue signal above an intensity threshold divided by the total number of green nuclei. The volumes of viral supernatant used in all subsequent infections were adjusted based on the differences between infection ratios.

Nuclear-green+ cytosolic red+ CRISPRi-i^{3}N iPSCs were passaged and plated at a density of 2.5x10^4 cells/well in Matrigel-coated 12-well culture plates. Shortly afterwards, the iPSCs were transduced with lentivirus containing individual sgRNAs. The following day, media was

changed to E8 + RI. Two days after infection, the media was changed to E8 + puromycin (12 ug/mL) to select for transduced cells.

Following selection for 3-4 additional days, the iPSCs were passaged into fresh Matrigel-coated 12-well culture plates at a high density and allowed to differentiate in Induction Medium with doxycycline (2 ug/mL) for 3 days, with daily media changes. Concurrently, the uninfected nuclear-green CRISPRi-i^{3}N iPSCs were differentiated alongside the infected nuclear-green+blue/cytosolic red CRISPRi-i^{3}N iPSCs.

Following the 3 days of differentiation, these partially-differentiated neurons were passaged and resuspended in Cortical Neuron Culture Medium with doxycycline (2 ug/uL), then plated on poly-L-ornithine-coated 96-well culture dishes (Perkin Elmer #6055308) at a density of 5.0×10^4 cells/well (n=6 wells per sgRNA for most, 3-5 for some). The nuclear-green+blue/cytosolic red CRISPRi-i^{3}Neurons were spiked in at a density of 1:20 with the nuclear-green CRISPRi-i^{3}Neurons to facilitate tracing of neurites while maintaining trophic support of higher-density neuron cultures. Following plating, we waited for adherence of neurons before imaging for the first time. For the remainder of each longitudinal imaging experiment, half of the culture medium was removed and an equal volume of fresh medium was added three times per week.

For each timepoint, CRISPRi-i^{3}Neurons were imaged with a spinning disk confocal microscope with a motorized stage (Nikon Eclipse Ti), controlled using Nikon Elements software. A 20X objective was used to acquire a series of 25 slightly overlapping images within each well followed by image stitching. Between imaging sessions, plates were incubated in a traditional water-jacketed 5% CO2 incubator at 37°C.

Longitudinal iPSC imaging

Nuclear-green CRISPRi-i^{3}N iPSCs were passaged and plated in Matrigel-coated 96-well culture dishes at a density of 1,000 cells/well. Following adherence, iPSCs were transduced with lentivirus (same preparation as for the longitudinal neuronal imaging) containing individual sgRNAs (n=3 wells per sgRNA). The following day, media was changed to E8 + ROCK inhibitor. Starting two days after infection, iPSCs were imaged with a spinning disk confocal microscope with a motorized stage (Nikon Eclipse Ti), controlled using Nikon Elements software. A 20X objective was used to acquire a series of 36 slightly overlapping images within each well followed by image stitching. Between imaging sessions, plates were incubated in a traditional water-jacketed 5% CO2 incubator at 37 ºC.

Bioinformatics analysis

Quant-Seq

Fastq files were uploaded to and processed through the cloud-based BlueBee Genomics Platform (https://www. bluebee.com/quantseq). Briefly, raw reads were trimmed with Bbduk, aligned with STAR Aligner, and counted with HTSeq-count to yield gene counts. Differential expression analyses were performed with the DESeq2 pipeline, which compared counts from each set of duplicates at different timepoints to counts from the day 0 timepoints. Additional, custom analysis pipelines were devised in R. We developed a simple web application with the Shiny R package that enables users to visualize normalized read counts and expression fold change

(relative to day 0) throughout neuronal differentiation for a queried gene. The web application can be accessed via kampmannlab.ucsf.edu/ineuron-rna-seq.

Primary screen.
We developed a bioinformatics pipeline, MAGeCK-iNC (MAGeCK including Negative Controls) for large-scale functional genomics analysis, which we made publicly available: (kampmannlab.ucsf.edu/mageck-inc). First, raw sequencing reads from next-generation sequencing were cropped and aligned to the reference using Bowtie (Langmead et al., 2009) to determine sgRNA counts in each sample. Next, counts files of two samples subject to comparison were input into MAGeCK and log2 fold changes (LFCs) and P values were calculated for each sgRNA using the 'mageck test –k' command. Following that, gene level knockdown phenotype scores were determined by averaging LFCs of the top 3 sgRNAs targeting this gene with the most significant P values. The statistical significance for each gene is determined by comparing the set of P values for sgRNAs targeting it with the set of P values for non-targeting control sgRNAs using the Mann-Whitney U test, as described previously (Kampmann et al., 2013, 2014). To correct for multiple hypothesis testing, we first performed random sampling of 5 with replacement from non-targeting control sgRNAs to generate 'pseudo-negative-control-genes' and calculated knockdown phenotype scores and P values for each of them. Then, we calculated the hit strength, defined as the product of knockdown phenotype score and –log (p value), for all genes in the library and for 'pseudo-negative-control-genes' generated above. Based on the distribution of all the products, a cutoff value was chosen to make sure the false-discovery rate (FDR) is less than 0.05. To find enriched annotations within hit genes, Gene Set Enrichment Analysis (GSEA) was performed for Day 10 iPSCs and Day 28 neurons using the fgsea package in R (Sergushichev, 2016).

Pooled validation screen.
sgRNA counts for each sample were determined as in primary screen. Subsequently, knockdown phenotype scores for each sgRNA were calculated as LFCs of sgRNA counts between two samples and were normalized by subtracting the median of non-targeting control sgRNAs. LFCs were averaged for samples with replicates. Gene-level knockdown phenotype score was determined as the mean of knockdown phenotype scores of all sgRNAs targeting this gene.

CROP-Seq.
Cell Ranger (version 2.2.0, 10X Genomics) with default parameters was used to align reads and generate digital expression matrices from single-cell sequencing data. To map sgRNA transcripts together with other mRNA transcripts to individual cells, a custom reference was generated by extending the human genome assembly (Ensembl GRCh38 release) with 'pseudo-genes' representing sgRNA-containing transcripts (one sgRNA sequence per pseudo-gene with 250bp upstream and 230bp downstream sequences). Sequencing results of sgRNA-enrichment libraries were analyzed using methods previously described (Hill et al., 2018) to further facilitate sgRNA identity assignment.

For a given cell, sgRNA(s) whose UMI counts were greater than 4 standard deviations of the mean UMI counts of all sgRNAs were assigned to that cell as its identity. Cells with only one assigned sgRNA were retained for further analysis. The Scater package (McCarthy et al., 2017) implemented in R was used to analyze the digital expression matrices including normalization, quality control and filtering.

The mean reads per cell was around 84,000 for iPSCs and 91,000 for neurons. Median number of genes detected per cell was around 5,000 for iPSCs and 4,600 for neurons. After quality control, a single sgRNA could be assigned to ~15,000 iPSCs and ~8,400 neurons

For each target gene, the top 50% cells with best on-target knockdown were retained. Differential gene expression analysis was performed between each gene knockdown group (cells assigned by targeting sgRNAs of that gene) and control group (cells assigned by non-targeting control sgRNAs) using the R package edgeR (Robinson et al., 2010) treating each cell as one replicate.

For Figure 4B, relative expression of each gene was calculated as *z*-normalized expression with respect to the mean and standard deviation of that gene in the control group:

$$x_{normalized} = \frac{x - \mu_{control}}{\sigma_{control}}$$

The top 20 most significantly altered genes were selected for each gene knockdown group and merged together to form the signature gene list. Gene knockdown groups were hierarchically clustered based on their relative expression of the signature genes.

For Figure 4F, GSEA was performed using the web tool WebGestalt (Zhang et al., 2005). For Figure 5A and S5A, the similarity score of transcriptome changes between two gene knockdown groups, A and B, was calculated as follows:

$$Similarity_{A,B} = \frac{|A_{up} \cap B_{up}| + |A_{down} \cap B_{down}|}{|A_{up} \cup B_{up}| + |A_{down} \cup B_{down}|}$$

A_{up} and B_{up} denote for the significantly upregulated genes (p_{adj}<0.01) in A and B, while A_{down} and B_{down} denote for the significantly downregulated genes (p_{adj}<0.01) in A and B.

Longitudinal imaging.

A CellProfiler (version 3.1.5) pipeline was developed to analyze longitudinal imaging data. For iPSC growth and i^3Neuron survival experiments, sgRNA+ cells were recognized as nuclear - green+ blue+ objects and the total number of sgRNA+ cells was quantified for every image. iPSC growth and i^3Neuron survival were calculated as the ratio of sgRNA+ cell number at different time points to that of day 1 of imaging. For neurite morphology analysis, neurites of sgRNA+ cells were first enhanced by the EnhanceOrSuppressFeatures and EnhanceEdges modules, and then skeletonized by the Morph module. Following that, MeasureObjectSkeleton module was implemented to measure neurite length, number of branches and number of trunks for individual neurons. The mean values of the above measurements of all sgRNA+ neurons were calculated for each image.

To integrate all image analysis data, we generated a panel of imaging phenotypes for a given sgRNA, including neurite length, number of neurite branches, number of neurite trunks, neuronal survival and iPSC growth at different time points. For Fig. 6G, the percentage changes of imaging phenotypes compared to the mean of non-targeting control sgRNAs were calculated for each sgRNA. Most of genes in the imaging experiment were targeted by two sgRNAs (some genes missed one sgRNA during experiment process), and a gene was discarded if it was targeted by two sgRNAs and the correlation of the two sgRNAs was less than 0.8. All remaining sgRNAs were hierarchically clustered based on the Pearson correlation of their percentage

changes of imaging phenotypes.

Table of oligonucleotide sequences

Name	Sequence	Use
B-actin For	ACCTTCTACAATGAGCTGCG	qPCR
B-actin Rev	CCTGGATAGCAACGTACATGG	qPCR
GAPDH For	ATGCCTCCTGCACCACCAAC	qPCR
GAPDH Rev	GGGGCCATCCACAGTCTTCT	qPCR
CDH2 For	CCCAAGACAAAGAGACCCAG	qPCR
CDH2 Rev	GCCACTGTGCTTACTGAATTG	qPCR
TFRC For	ACTTGCCCAGATGTTCTCAG	qPCR
TFRC Rev	GTATCCCTCTAGCCATTCAGTG	qPCR
GRN For	TCCAGAGTAAGTGCCTCTCCA	qPCR
GRN Rev	TCACCTCCATGTCACATTTCA	qPCR
Enrichment_PCR_1_For	TCGCACGGACTTGTGGGAGAAG	sgRNA enrichment PCR
Enrichment_PCR_1_Rev	CTACACGACGCTCTTCCGATCT	sgRNA enrichment PCR
Enrichment_PCR_2_For	GTGACTGGAGTTCAGACGTGTG CTCTTCCGATCTAGTATCCCTTG GAGAACCACCTTG	sgRNA enrichment PCR
Enrichment_PCR_2_Rev	AATGATACGGCGACCACCGA-GATCTACACTCTTTCCCTACAC GACGCTC	sgRNA enrichment PCR
Enrichment_PCR_3_For	CAAGCAGAAGACGGCATACGA GAT-**[index]**-GTGACTGGAGTTCAG	sgRNA enrichment PCR

SUPPLEMENTAL INFORMATION TITLES AND LEGENDS

Supplemental Figure S1. Normal karyotype and CRISPRi activity of the CRISPRi- i^3N iPSC monoclonal line (related to Fig. 1)

(A) Karyotyping of the monoclonal CRISPRi- i^3N iPSC line confirmed a normal male karyotype.

(B) Knockdown of N-cadherin (*CDH2*) in iPSC-derived neurons monitored on the protein level by immunofluorescence (IF) microscopy. White arrows mark cells infected with a lentiviral plasmid expressing an sgRNA and GFP (green). *Top row*, uninfected cells. *Middle row*, non-targeting negative control sgRNA. N-cadherin signal (IF, red) is similar in infected and uninfected cells. *Bottom row*, sgRNA targeting N-cadherin (*CDH2*). For the infected cells, N-cadherin signal (IF, red) is substantially reduced compared with neighboring uninfected cells. Nuclear counterstain DAPI is shown in blue.

Supplemental Figure S2. Characterization of results from massively parallel screens for essential genes in iPSCs and neurons (related to Fig. 2)

(A) Correlation of read counts from next-generation sequencing for individual sgRNAs between experimental replicates.

(B) Volcano plots summarizing knockdown phenotypes and statistical significance (Mann-Whitney U test) for genes targeted in the pooled screen in iPSC-derived neurons. *Top*, phenotypes for survival between Day 0 and Day 14. *Bottom*, phenotypes for survival between Day 0 and Day 21. Dashed lines represent the cutoff for hit genes, which was defined based on the product of phenotype and $-\log_{10}$(P value) at an empirically determined false discovery rate of 0.05 (see Methods).

(C) Gene set enrichment analysis (GSEA) for hit genes from the screens. Significantly enriched GO terms for biological processes (BH-adjusted P value<0.05: 100,000 permutations) are shown for essential genes in iPSCs (Day 0 vs. Day 10) and neurons (Day 0 vs. Day 28). NES, normalized enrichment score.

(D) Expression levels of essential and non-essential genes in neurons at Day 14, 21, and 28 of differentiation were plotted as the distributions of $\log_{10}$ normalized counts from Quant-Seq. Median levels of expression were indicated. P values were calculated using one-sided Mann-Whitney U test.

Supplemental Figure S3. Pooled validation of hit genes from the primary screen (related to Fig. 3)

(A) Heatmap showing relative knockdown phenotype scores of sgRNAs (columns) from the validation screens (rows, both experimental replicates, expect for Day 28neurons, for which the

second replicate sample was accidentally lost during sample preparation). Both sgRNAs and screens were hierarchically clustered based on Pearson correlation.

(B) Construct pMTL5 for the expression of CRISPRi machinery (dCas9-BFP-KRAB) fused to an N-terminal DHFR degrons from the AAVS1 safe-harbor locus.

(C) Characterization of inducible CRISPRi activity in iPSCs with integrated single-degron CRISPRi machinery (construct pMTL5), compared to an equivalent constitutive construct lacking the degron (pMTL3). iPSCs were transduced with a lentiviral sgRNA expression construct containing a non-targeting sgRNA (grey bars) or an sgRNA targeting *CDH2* (encoding N-cadherin, blue bars). Cells were cultured in the presence or absence of 10 μM trimethoprim (TMP), and cell-surface levels of N-cadherin were quantified by immunofluorescence flow cytometry 48 hours after transduction. Expression levels relative to non-targeting sgRNA are shown. Mean of two experimental replicates, error bars indicate standard deviation.

(D,E) Characterization of inducible CRISPRi activity in iPSCs and neurons with integrated double-degron CRISPRi machinery (construct pRT029). (D) Knockdown of the transferrin receptor (*TFRC*) in iPSCs and iPSC-derived neurons in the presence or absence of trimethoprim (TMP). iPSCs expressing the inducible CRISPRi machinery were lentivirally infected with an sgRNA targeting *TFRC* or a non-targeting negative control sgRNA. Infected iPSCs were cultured and differentiated into neurons in the presence of 20 μM TMP from iPSC stage or in the absence of TMP. Cells from both conditions were harvested at different days and levels of *TFRC* as well as *ACTB* mRNAs were quantified by qPCR. After normalizing each sample by *ACTB* mRNA levels, ratios of *TFRC* mRNA were calculated for cells expressing the *TFRC*-targeting sgRNA versus cells with the non-targeting sgRNA cultured in the same condition. Mean and standard deviations for replicates are shown. (E) qPCR result showing the conditional knockdown of *GRN* in iPSC-derived neurons. iPSCs expressing the dual-degron inducible CRISPRi machinery were lentivirally infected with an sgRNA targeting *GRN* or a non-targeting negative control sgRNA. Infected iPSCs were differentiated into neurons. The neurons were cultured in neuronal medium with the presence or absence of 20 μM TMP. Day 7 neurons from both conditions were harvested and levels of *GRN* as well as *ACTB* mRNAs were quantified by qPCR. After normalizing each sample by *ACTB* mRNA levels, ratios of *GRN* mRNA were calculated for cells expressing the *GRN*-targeting sgRNA versus cells with the control sgRNA cultured in the same condition. Mean and standard deviations for replicates are shown. One-tailed t-test was applied (*** $P<0.001$).

(**F,G**) Inhibition of the neuronal differentiation of CRISPRi-i^{3}N iPSCs by sgRNAs targeting *PPP1R12C*. (F) Phase contrast (first column) and fluorescence (second and third column) micrographs of partially differentiated neuron populations infected with an expression construct for sgRNAs (non-targeting control sgRNA, top row, or two different sgRNAs targeting *PPP1R12C*, middle and bottom row) and a BFP marker. Nuclei are visualized by expression of mNeonGreen-NLS (second column, green in merged images). Cells expressing sgRNAs are marked by cytosolic BFP (third column, blue in merged images). Images were acquired following six days of iPSC proliferation post-infection and three days of doxycycline-induced differentiation. (G) Quantification of undifferentiated colonies in a repeat experiment. Rosettes were counted manually by an individual blinded to the experimental conditions. The total

number of cells was counted by Nikon Elements software bright spot detection module for green nuclei. Mean and SEM for replicate wells are shown (n = 6). One-way ANOVA and multiple comparisons were applied (****P<0.0001).

Supplemental Fig. S4. Characterization of CROP-Seq screen results (related to Fig. 4)

(**A**) Transcriptomes of different sgRNA groups in iPSCs (left) and neurons (right) were visualized with t-Distributed stochastic neighbor embedding (t-SNE), colored by target genes.

(**B**) On-target knockdown efficiencies in the CROP-Seq screen were quantified for iPSCs (left) and Day 7 neurons (right). For each target gene, the 50% of cells with the strongest on-target knockdown were selected from all cells expressing sgRNAs targeting the gene. This group of cells was called the "gene knockdown group". Average expression of each target gene is compared between cells with non-targeting control sgRNAs and cells within the gene knockdown group (top panels). Average percentage of remaining mRNA relative to non-targeting control cells was quantified for each gene knockdown group (bottom panels). Error bars represent 95% confidence intervals estimated by bootstrapping.

Supplemental Fig. S5. Differential transcriptomic consequences of gene knockdown in iPSCs and neurons (related to Fig. 5)

(**A**) Pairwise similarities of transcriptome changes of different gene knockdown groups across iPSCs and neurons were determined based on the numbers of overlapping and total transcripts that were significantly altered in two groups (see Methods for details). Gene knockdown groups were hierarchically clustered based on Pearson correlations. The darkness of red color indicates the value of similarity.

(**B,C**) MA plots showing transcriptomic changes caused by knockdown of (B) *UQCRQ* or (C) *UBA1* in iPSCs and iPSC-derived neurons. Results from the CROP-Seq screen, gene expression differences for gene knockdown groups relative to the negative control group. Differentially expressed genes ($p_{adj} < 0.05$) were colored red (upregulation) or blue (downregulation), and selected genes of interest were labeled.

Supplemental Fig. S6. Reproducibility of longitudinal imaging results (related to Fig. 6)

Scatter plot showing surviving fractions of neurons with different sgRNAs at different days of differentiation (shown in different colors) relative to Day 1 in two replicate imaging experiments. Each dot represents one sgRNA in a certain time point. Coefficient of determination (R^2) is indicated.

Supplemental Table S1. Phenotypes from the primary screen (related to Fig. 2)
Phenotypes from the primary screens (Day 10 iPSCs, Day 14 neurons, Day 21 neurons, Day 28 neurons) are listed for all genes targeted H1 library (see Methods for details). Columns are:

Targeted transcription start site, targeted gene, Knockdown phenotype, P value, and the product of phenotype x –log10(P value).

Supplemental Table S2. Pooled validation screen sgRNAs and phenotypes (related to Fig. 3)
Protospacer sequences and phenotypes from the validation screens are listed for all sgRNAs from the pooled validation library (see Methods for details). Columns are: sgRNA short name (as used throughout the study), sgRNA long names (from the original H1 library), protospacer sequences, and phenotypes from the different screens in the following columns.

Supplemental Table S3. Differentially expressed genes from the CROP-Seq screen (related to Fig. 4)
The table provides the numerical values underlying the heatmaps in Fig. 4B. Columns: genes targeted by CRISPRi. Rows: differentially expressed genes. See Methods for details.

Supplemental Table S4. Gene expression changes in neurons in response to *MAT2A* and *MAP3K12* knockdown (related to Fig. 4 and 5)
The table lists changes in gene expression for *MAP3K12* or *MAT2A* knockdown versus nontargeting sgRNA neurons (see Methods for details).

Supplemental Movie S1. Time-lapse of longitudinal imaging for iPSC-derived neurons expressing a non-targeting control sgRNA (related to Fig. 6)
The ten frames represent Days 1, 2, 3, 4, 5, 6, 8, 10, 13, and 16 of imaging. Red: cytosolic mScarlet. Blue: nuclear-localized BFP marker from sgRNA construct. The movie is shown at a speed of 4 fps.

Supplemental Movie S2. Time-lapse of longitudinal imaging for iPSC-derived neurons expressing a sgRNA targeting *UQCRQ* (related to Fig. 6)
The ten frames represent Days 1, 2, 3, 4, 5, 6, 8, 10, 13, and 16 of imaging. Red: cytosolic mScarlet. Blue: nuclear-localized BFP marker from sgRNA construct. The movie is shown at a speed of 4 fps.

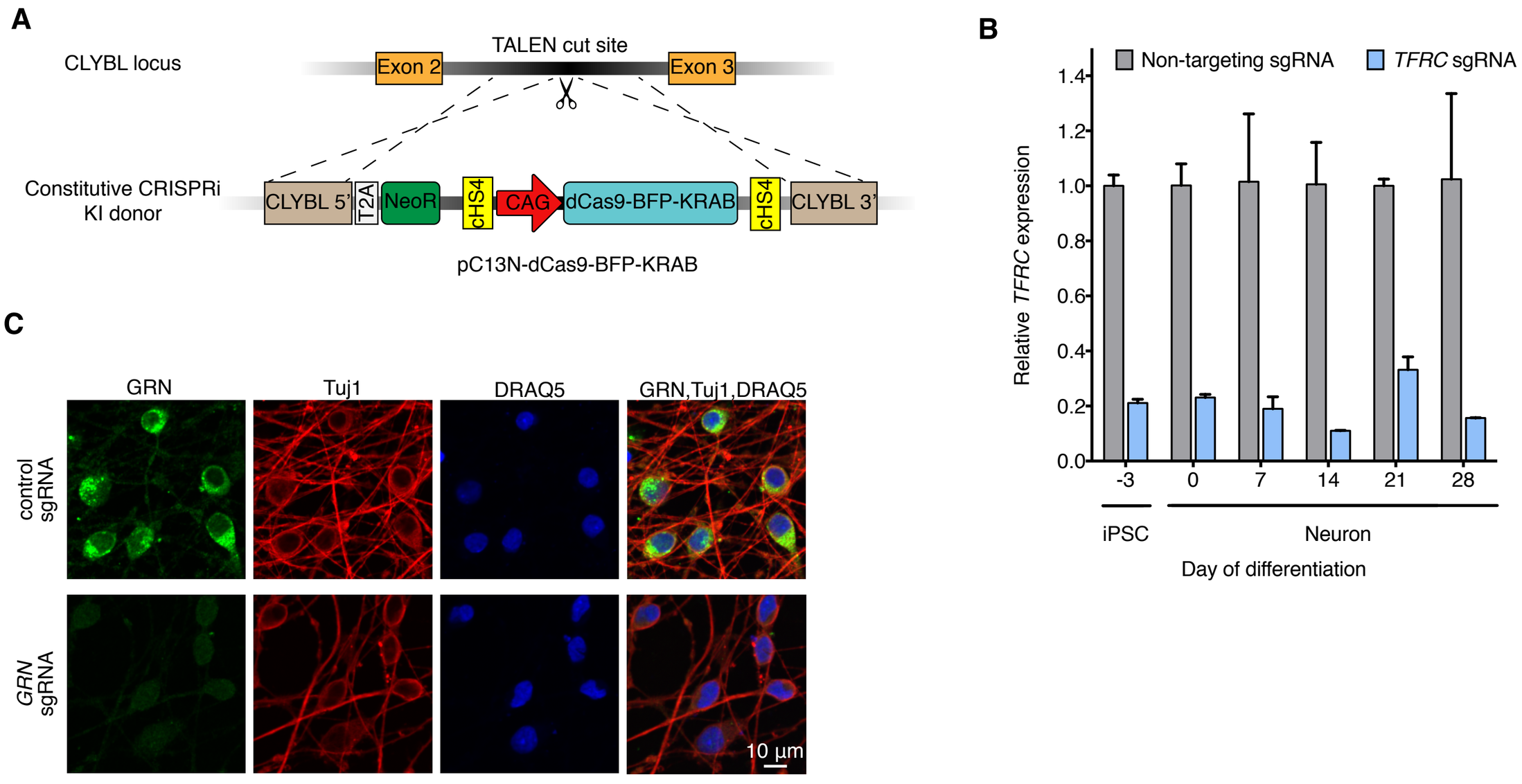
A
CLYBL locus
TALEN cut site
Exon 2
Exon 3
Constitutive CRISPRi
KI donor
CLYBL 5'
T2A
NeoR
cHS4
CAG
dCas9-BFP-KRAB
cHS4
CLYBL 3'
pC13N-dCas9-BFP-KRAB
B
Non-targeting sgRNA
TFRC sgRNA
Relative TFRC expression
1.4
1.2
1.0
0.8
0.6
0.4
0.2
0.0
-3
0
7
14
21
28
iPSC
Neuron
Day of differentiation
C
GRN
Tuj1
DRAQ5
GRN,Tuj1,DRAQ5
control sgRNA
GRN sgRNA
10 µm

Figure 1

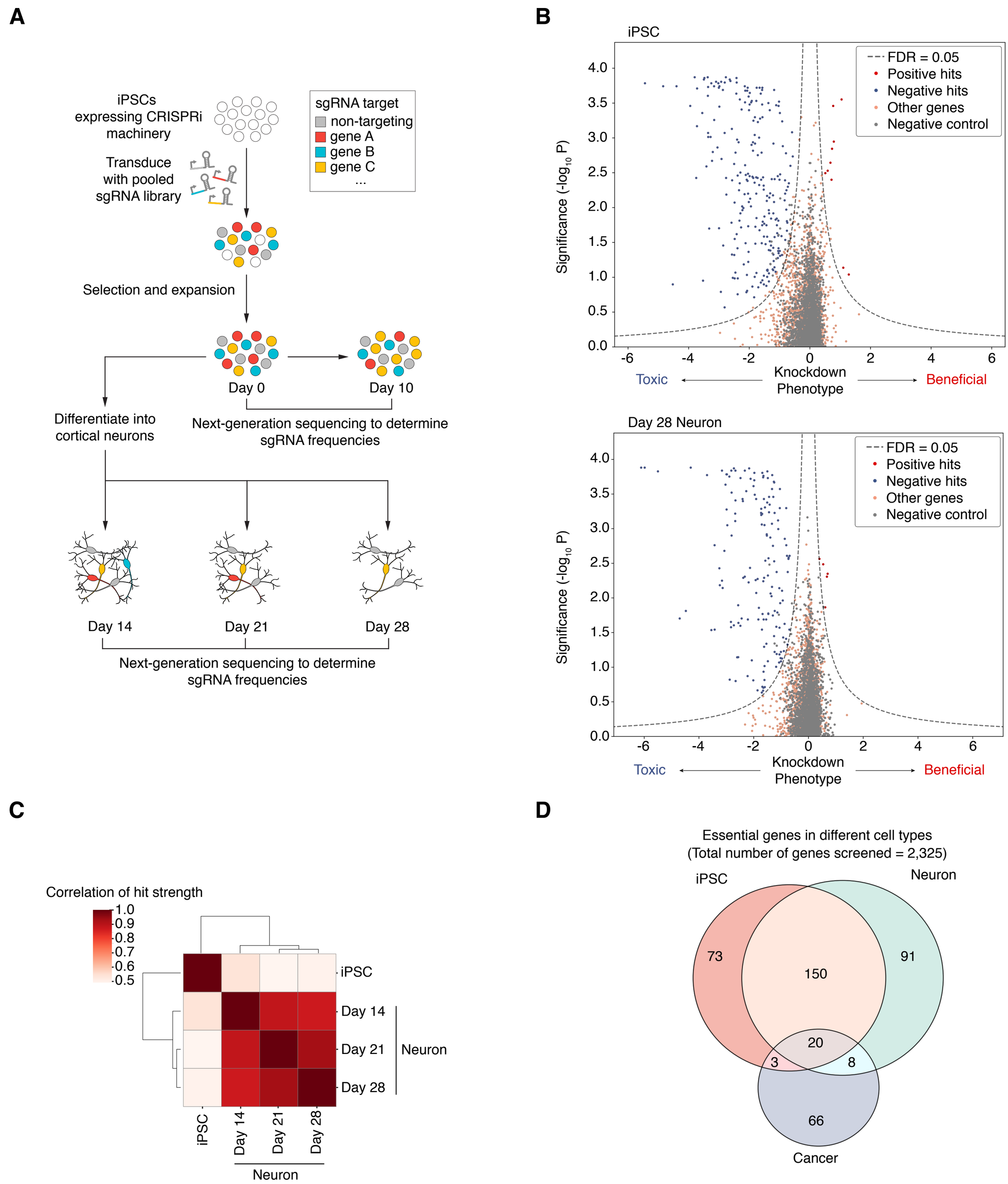
A
iPSCs expressing CRISPRi machinery
Transduce with pooled sgRNA library
sgRNA target
non-targeting
gene A
gene B
gene C
...
Selection and expansion
Day 0
Day 10
Differentiate into cortical neurons
Next-generation sequencing to determine sgRNA frequencies
Day 14
Day 21
Day 28
Next-generation sequencing to determine sgRNA frequencies
B
iPSC
FDR = 0.05
Positive hits
Negative hits
Other genes
Negative control
Significance (-log10 P)
Knockdown Phenotype
Toxic
Beneficial
Day 28 Neuron
C
Correlation of hit strength
iPSC
Day 14
Day 21
Day 28
Neuron
D
Essential genes in different cell types
(Total number of genes screened = 2,325)
iPSC
Neuron
Cancer
73
150
91
20
3
8
66

Figure 2

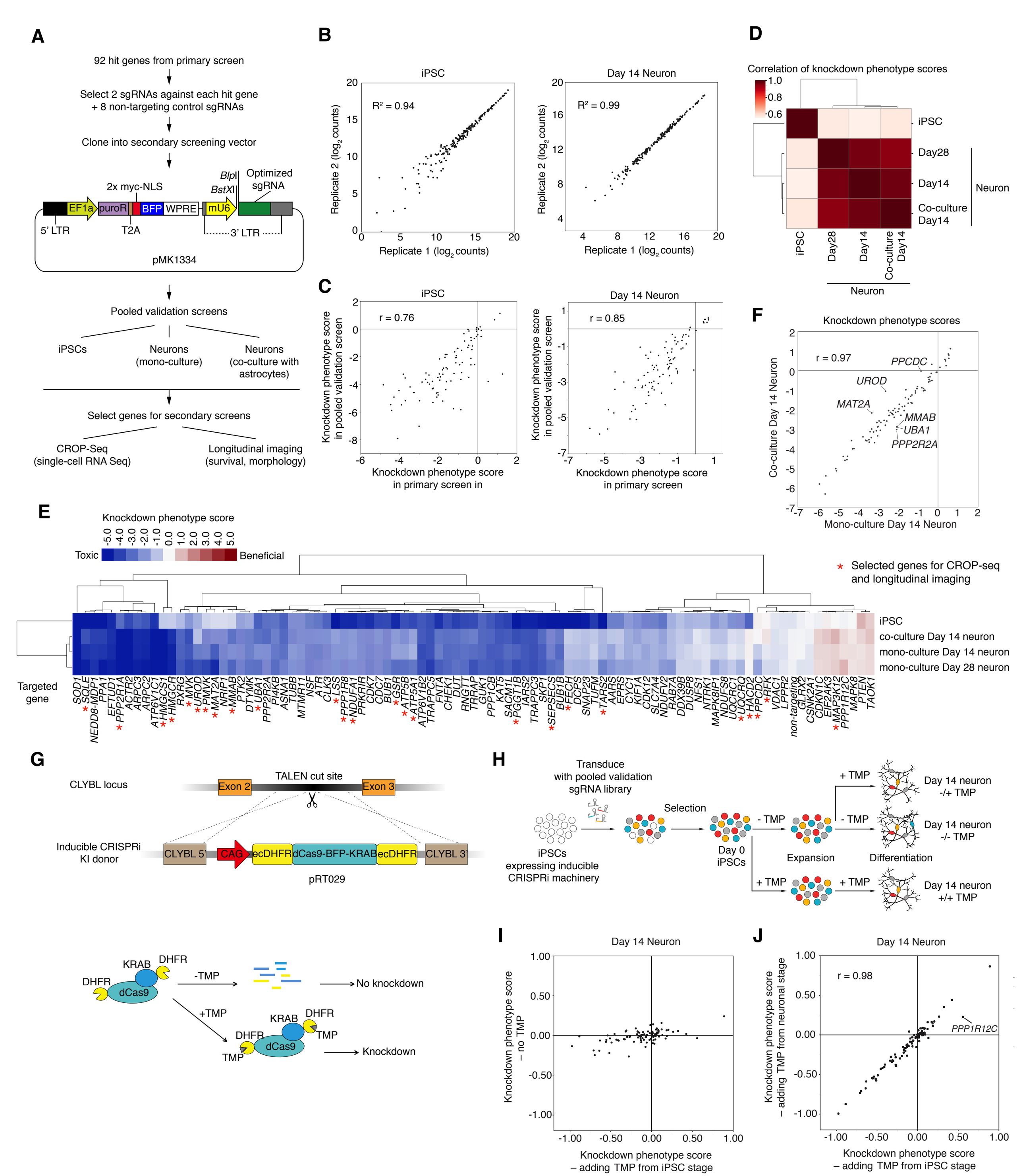
A
92 hit genes from primary screen
Select 2 sgRNAs against each hit gene + 8 non-targeting control sgRNAs
Clone into secondary screening vector
2x myc-NLS
BlpI
BstXI
Optimized sgRNA
EF1a
puroR
BFP
WPRE
mU6
5' LTR
T2A
3' LTR
pMK1334
Pooled validation screens
iPSCs
Neurons (mono-culture)
Neurons (co-culture with astrocytes)
Select genes for secondary screens
CROP-Seq (single-cell RNA Seq)
Longitudinal imaging (survival, morphology)
B
iPSC
R² = 0.94
Day 14 Neuron
R² = 0.99
Replicate 1 (log2 counts)
Replicate 2 (log2 counts)
C
iPSC
r = 0.76
Day 14 Neuron
r = 0.85
Knockdown phenotype score in pooled validation screen
Knockdown phenotype score in primary screen in
D
Correlation of knockdown phenotype scores
iPSC
Day28
Day14
Co-culture Day14
Neuron
E
Knockdown phenotype score
Toxic
Beneficial
Selected genes for CROP-seq and longitudinal imaging
iPSC
co-culture Day 14 neuron
mono-culture Day 14 neuron
mono-culture Day 28 neuron
Targeted gene
F
Knockdown phenotype scores
r = 0.97
PPCDC
UROD
MAT2A
MMAB
UBA1
PPP2R2A
Co-culture Day 14 Neuron
Mono-culture Day 14 Neuron
G
CLYBL locus
TALEN cut site
Exon 2
Exon 3
Inducible CRISPRi KI donor
CLYBL 5'
CAG
ecDHFR
dCas9-BFP-KRAB
ecDHFR
CLYBL 3'
pRT029
KRAB
DHFR
dCas9
-TMP
No knockdown
+TMP
TMP
Knockdown
H
Transduce with pooled validation sgRNA library
iPSCs expressing inducible CRISPRi machinery
Selection
Day 0 iPSCs
- TMP
+ TMP
Expansion
Differentiation
Day 14 neuron -/+ TMP
Day 14 neuron -/- TMP
Day 14 neuron +/+ TMP
I
Day 14 Neuron
Knockdown phenotype score – no TMP
Knockdown phenotype score – adding TMP from iPSC stage
J
Day 14 Neuron
r = 0.98
PPP1R12C
Knockdown phenotype score – adding TMP from neuronal stage
Knockdown phenotype score – adding TMP from iPSC stage

Figure 3

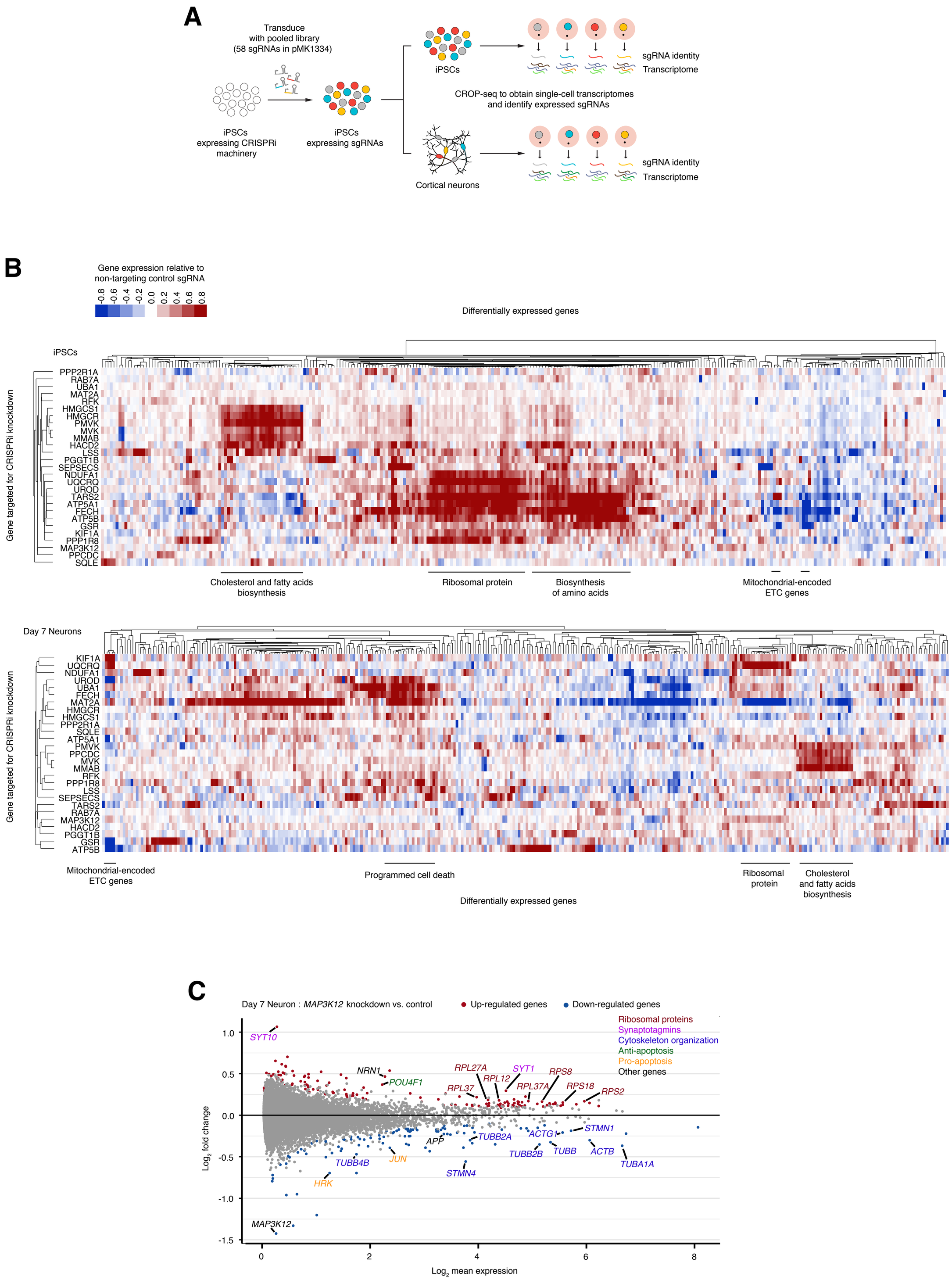
A
Transduce
with pooled library
(58 sgRNAs in pMK1334)
iPSCs
expressing CRISPRi
machinery
iPSCs
expressing sgRNAs
iPSCs
sgRNA identity
Transcriptome
CROP-seq to obtain single-cell transcriptomes
and identify expressed sgRNAs
Cortical neurons
sgRNA identity
Transcriptome
B
Gene expression relative to
non-targeting control sgRNA
-0.8 -0.6 -0.4 -0.2 0.0 0.2 0.4 0.6 0.8
Differentially expressed genes
iPSCs
Gene targeted for CRISPRi knockdown
PPP2R1A
RAB7A
UBA1
MAT2A
RFK
HMGCS1
HMGCR
PMVK
MVK
MMAB
HACD2
LSS
PGGT1B
SEPSECS
NDUFA1
UQCRQ
UROD
TARS2
ATP5A1
FECH
ATP5B
GSR
KIF1A
PPP1R8
MAP3K12
PPCDC
SQLE
Cholesterol and fatty acids
biosynthesis
Ribosomal protein
Biosynthesis
of amino acids
Mitochondrial-encoded
ETC genes
Day 7 Neurons
Gene targeted for CRISPRi knockdown
KIF1A
UQCRQ
NDUFA1
UROD
UBA1
FECH
MAT2A
HMGCR
HMGCS1
PPP2R1A
SQLE
ATP5A1
PMVK
PPCDC
MVK
MMAB
RFK
PPP1R8
LSS
SEPSECS
TARS2
RAB7A
MAP3K12
HACD2
PGGT1B
GSR
ATP5B
Mitochondrial-encoded
ETC genes
Programmed cell death
Ribosomal
protein
Cholesterol
and fatty acids
biosynthesis
Differentially expressed genes
C
Day 7 Neuron : MAP3K12 knockdown vs. control
Up-regulated genes
Down-regulated genes
Ribosomal proteins
Synaptotagmins
Cytoskeleton organization
Anti-apoptosis
Pro-apoptosis
Other genes
SYT10
NRN1
POU4F1
RPL27A
RPL12
RPL37
SYT1
RPL37A
RPS8
RPS18
RPS2
STMN1
ACTG1
TUBB2A
APP
TUBB2B
TUBB
ACTB
TUBA1A
TUBB4B
JUN
STMN4
HRK
MAP3K12
1.0
0.5
0.0
-0.5
-1.0
-1.5
Log2 fold change
0
2
4
6
8
Log2 mean expression

Figure 4

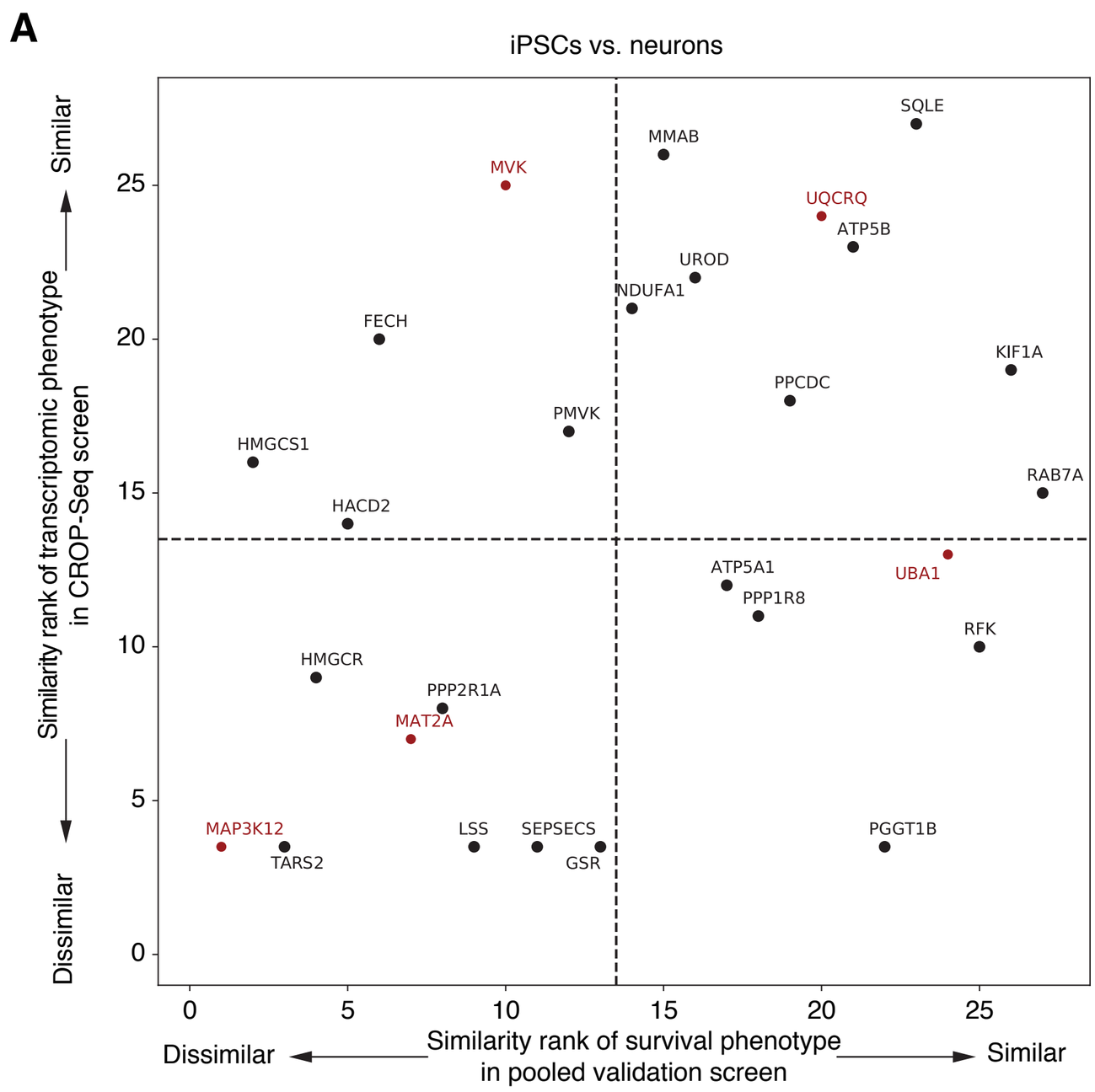
A
iPSCs vs. neurons
Similarity rank of transcriptomic phenotype in CROP-Seq screen
Similar
Dissimilar
Similarity rank of survival phenotype in pooled validation screen
Dissimilar
Similar
SQLE
MMAB
MVK
UQCRQ
ATP5B
UROD
NDUFA1
FECH
KIF1A
PPCDC
PMVK
HMGCS1
RAB7A
HACD2
ATP5A1
UBA1
PPP1R8
RFK
HMGCR
PPP2R1A
MAT2A
MAP3K12
TARS2
LSS
SEPSECS
GSR
PGGT1B

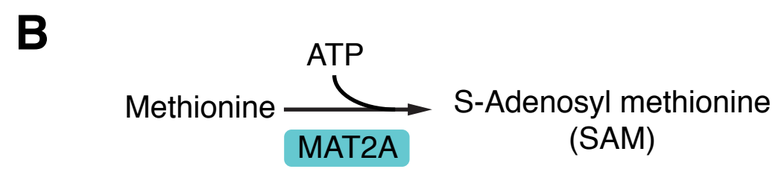
B
ATP
Methionine
MAT2A
S-Adenosyl methionine (SAM)

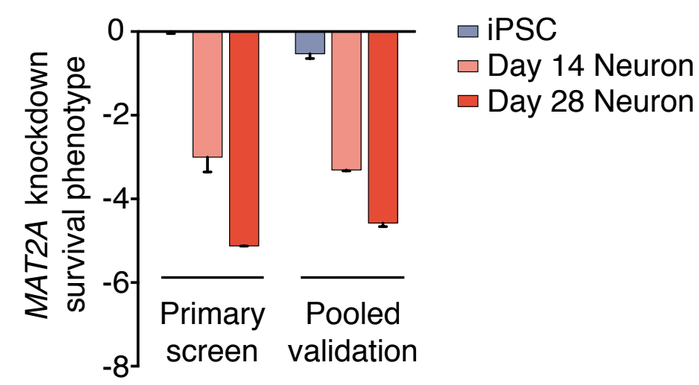
C
MAT2A knockdown survival phenotype
iPSC
Day 14 Neuron
Day 28 Neuron
Primary screen
Pooled validation

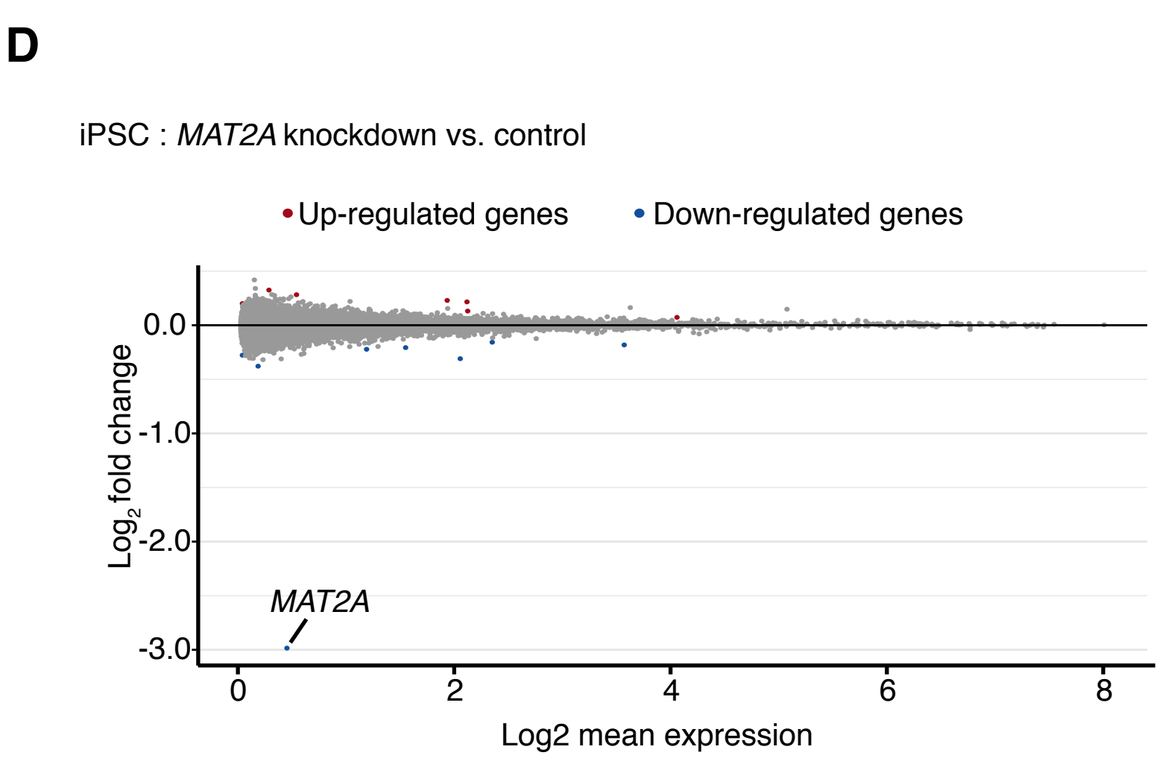
D
iPSC : MAT2A knockdown vs. control
Up-regulated genes
Down-regulated genes
Log2 fold change
MAT2A
Log2 mean expression

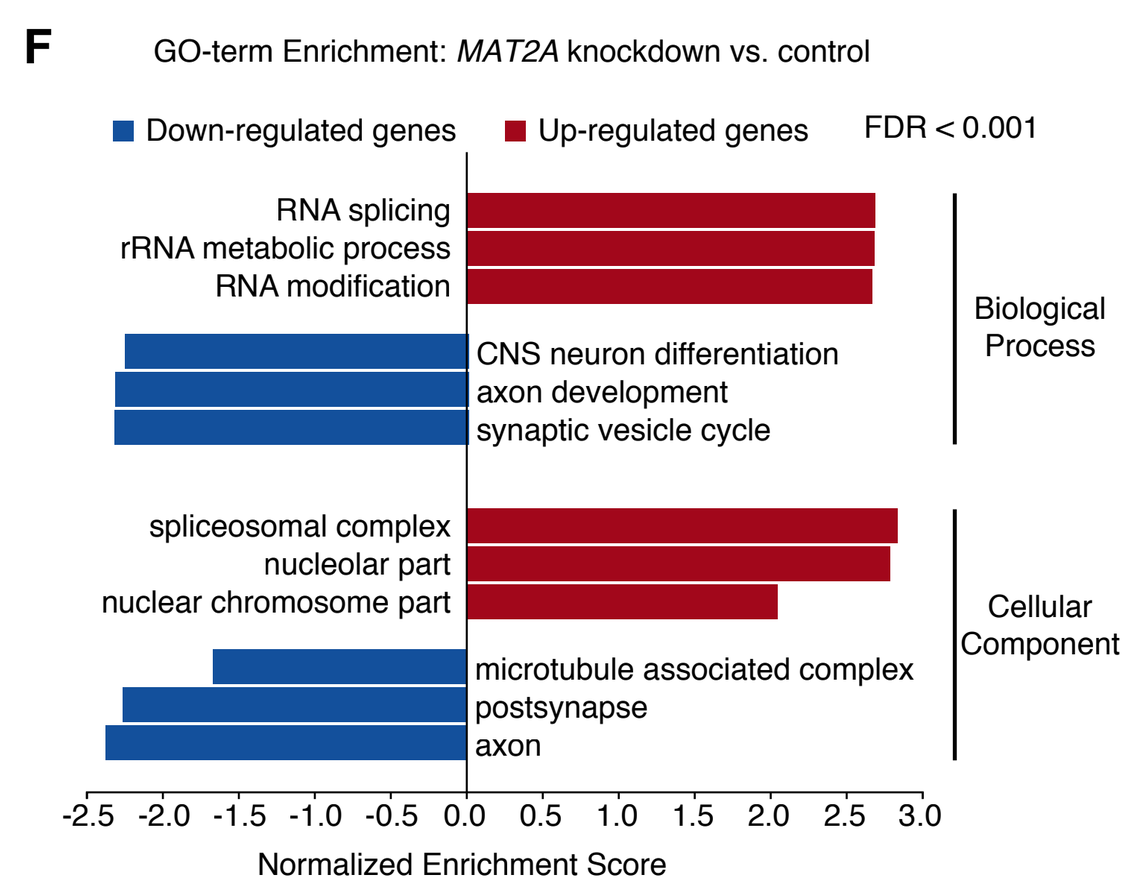
F
GO-term Enrichment: MAT2A knockdown vs. control
Down-regulated genes
Up-regulated genes
FDR < 0.001
RNA splicing
rRNA metabolic process
RNA modification
CNS neuron differentiation
axon development
synaptic vesicle cycle
Biological Process
spliceosomal complex
nucleolar part
nuclear chromosome part
microtubule associated complex
postsynapse
axon
Cellular Component
Normalized Enrichment Score

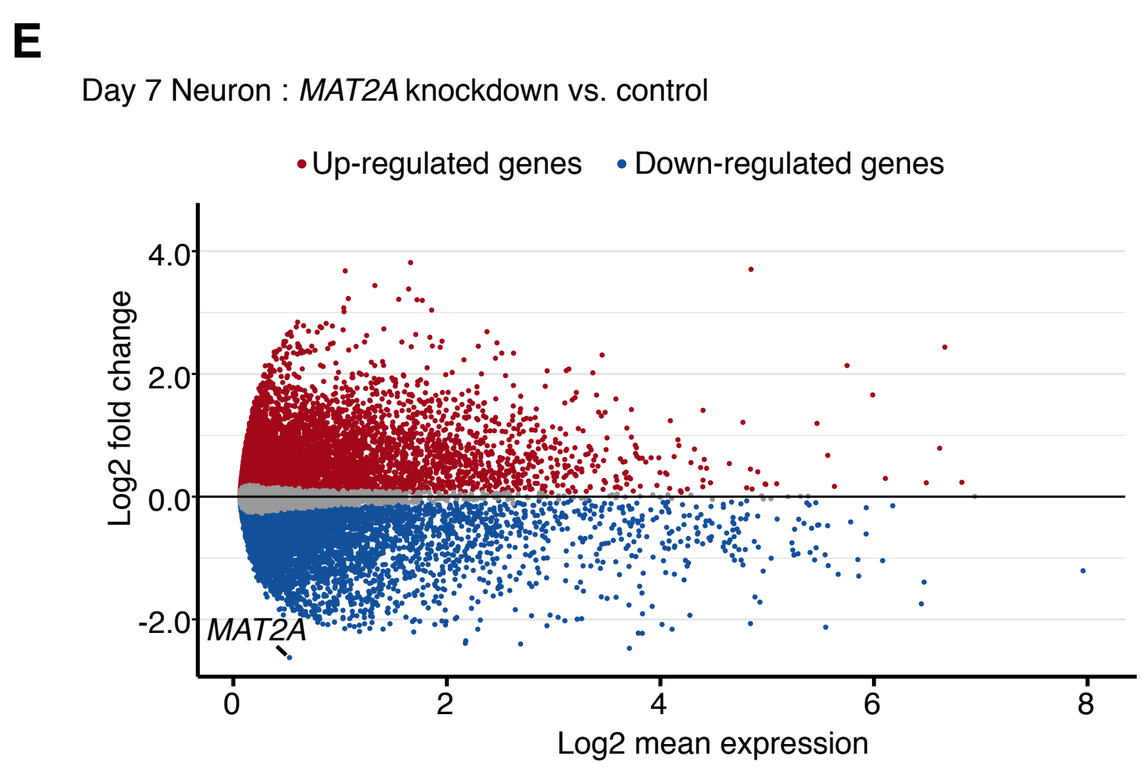
E
Day 7 Neuron : MAT2A knockdown vs. control
Up-regulated genes
Down-regulated genes
Log2 fold change
MAT2A
Log2 mean expression

Figure 5

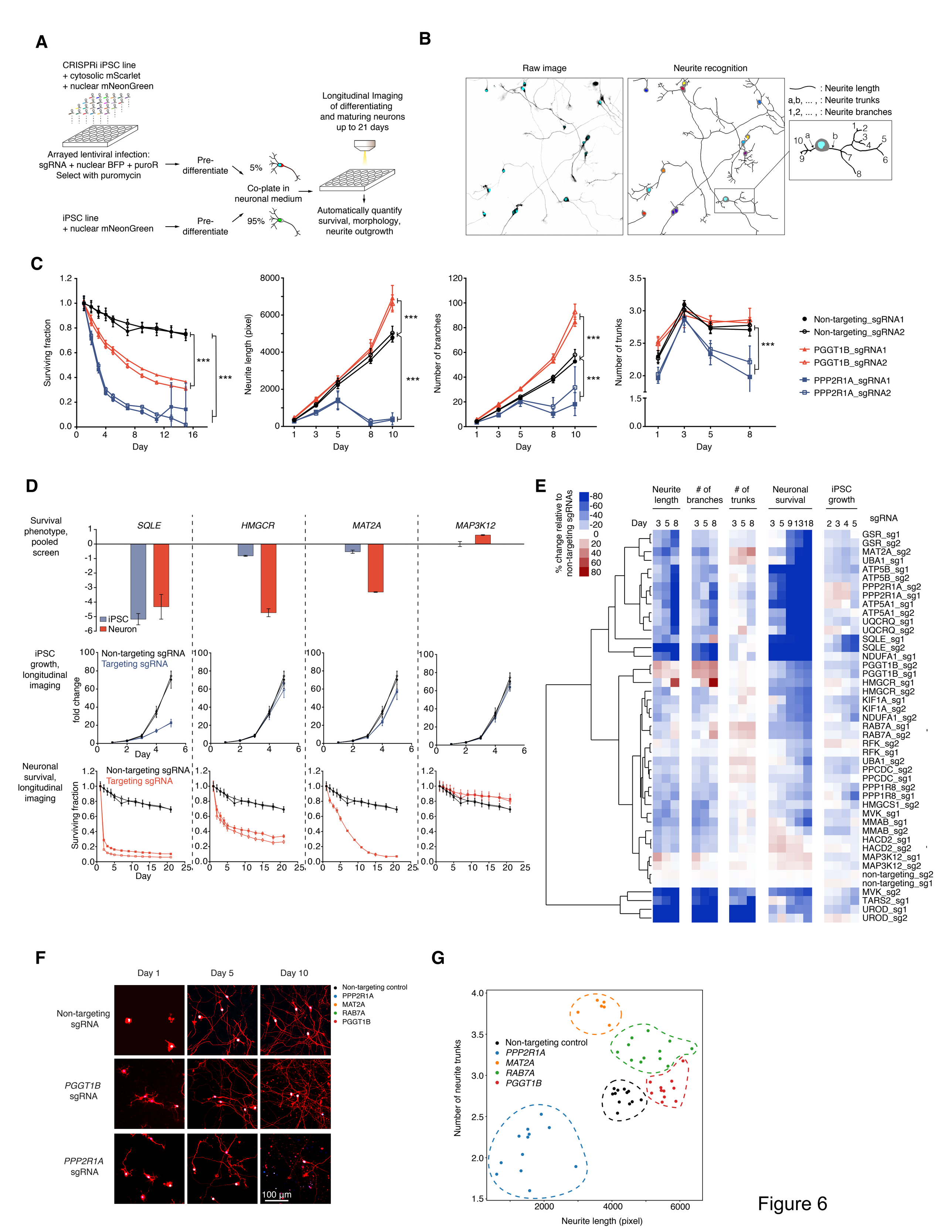
A
CRISPRi iPSC line
+ cytosolic mScarlet
+ nuclear mNeonGreen
Arrayed lentiviral infection:
sgRNA + nuclear BFP + puroR
Select with puromycin
Pre-differentiate
5%
Co-plate in neuronal medium
iPSC line
+ nuclear mNeonGreen
Pre-differentiate
95%
Longitudinal Imaging of differentiating and maturing neurons up to 21 days
Automatically quantify survival, morphology, neurite outgrowth
B
Raw image
Neurite recognition
: Neurite length
a,b, ... , : Neurite trunks
1,2, ... , : Neurite branches
C
Surviving fraction
Neurite length (pixel)
Number of branches
Number of trunks
Day
Non-targeting_sgRNA1
Non-targeting_sgRNA2
PGGT1B_sgRNA1
PGGT1B_sgRNA2
PPP2R1A_sgRNA1
PPP2R1A_sgRNA2
D
Survival phenotype, pooled screen
SQLE
HMGCR
MAT2A
MAP3K12
iPSC
Neuron
iPSC growth, longitudinal imaging
Non-targeting sgRNA
Targeting sgRNA
fold change
Neuronal survival, longitudinal imaging
Surviving fraction
Day
E
% change relative to non-targeting sgRNAs
Neurite length
# of branches
# of trunks
Neuronal survival
iPSC growth
Day
sgRNA
GSR_sg1
GSR_sg2
MAT2A_sg2
UBA1_sg1
ATP5B_sg1
ATP5B_sg2
PPP2R1A_sg2
PPP2R1A_sg1
ATP5A1_sg1
ATP5A1_sg2
UQCRQ_sg1
UQCRQ_sg2
SQLE_sg1
SQLE_sg2
NDUFA1_sg1
PGGT1B_sg2
PGGT1B_sg1
HMGCR_sg1
HMGCR_sg2
KIF1A_sg1
KIF1A_sg2
NDUFA1_sg2
RAB7A_sg1
RAB7A_sg2
RFK_sg2
RFK_sg1
UBA1_sg2
PPCDC_sg2
PPCDC_sg1
PPP1R8_sg2
PPP1R8_sg1
HMGCS1_sg2
MVK_sg1
MMAB_sg1
MMAB_sg2
HACD2_sg1
HACD2_sg2
MAP3K12_sg1
MAP3K12_sg2
non-targeting_sg2
non-targeting_sg1
MVK_sg2
TARS2_sg1
UROD_sg1
UROD_sg2
F
Day 1
Day 5
Day 10
Non-targeting sgRNA
PGGT1B sgRNA
PPP2R1A sgRNA
Non-targeting control
PPP2R1A
MAT2A
RAB7A
PGGT1B
100 µm
G
Non-targeting control
PPP2R1A
MAT2A
RAB7A
PGGT1B
Number of neurite trunks
Neurite length (pixel)

Figure 6

A CRISPRi-i_3 N iPSC monoclonal line

B

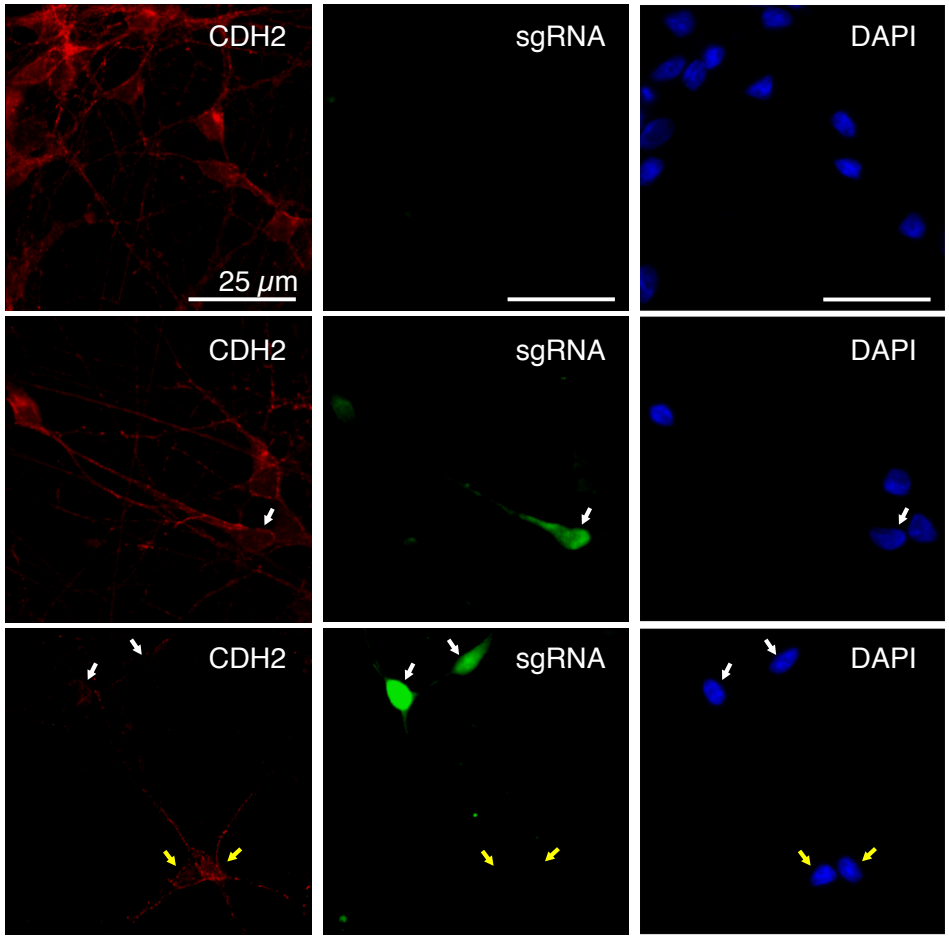

Supplemental Fig. S1

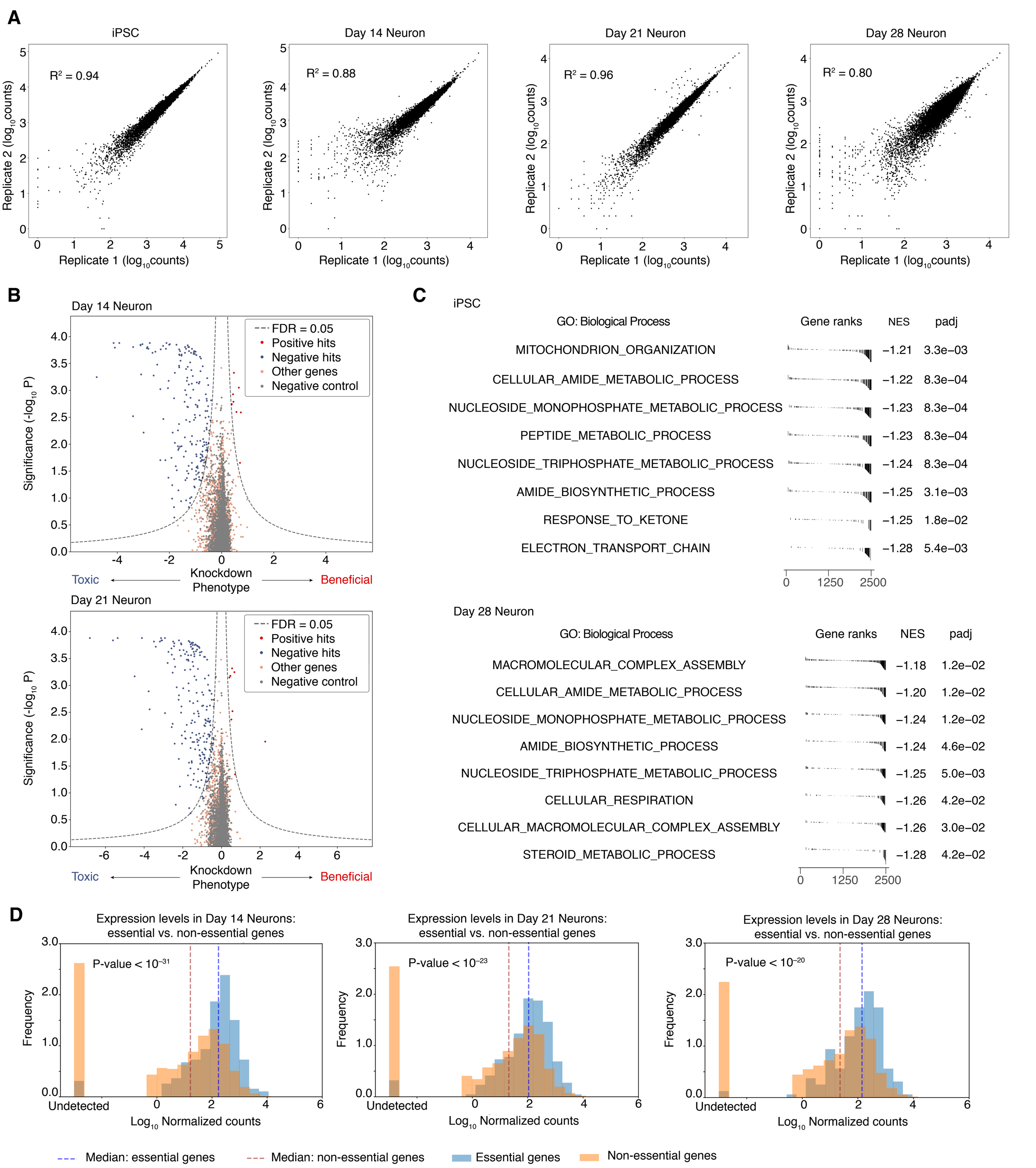

Supplemental Fig. S2

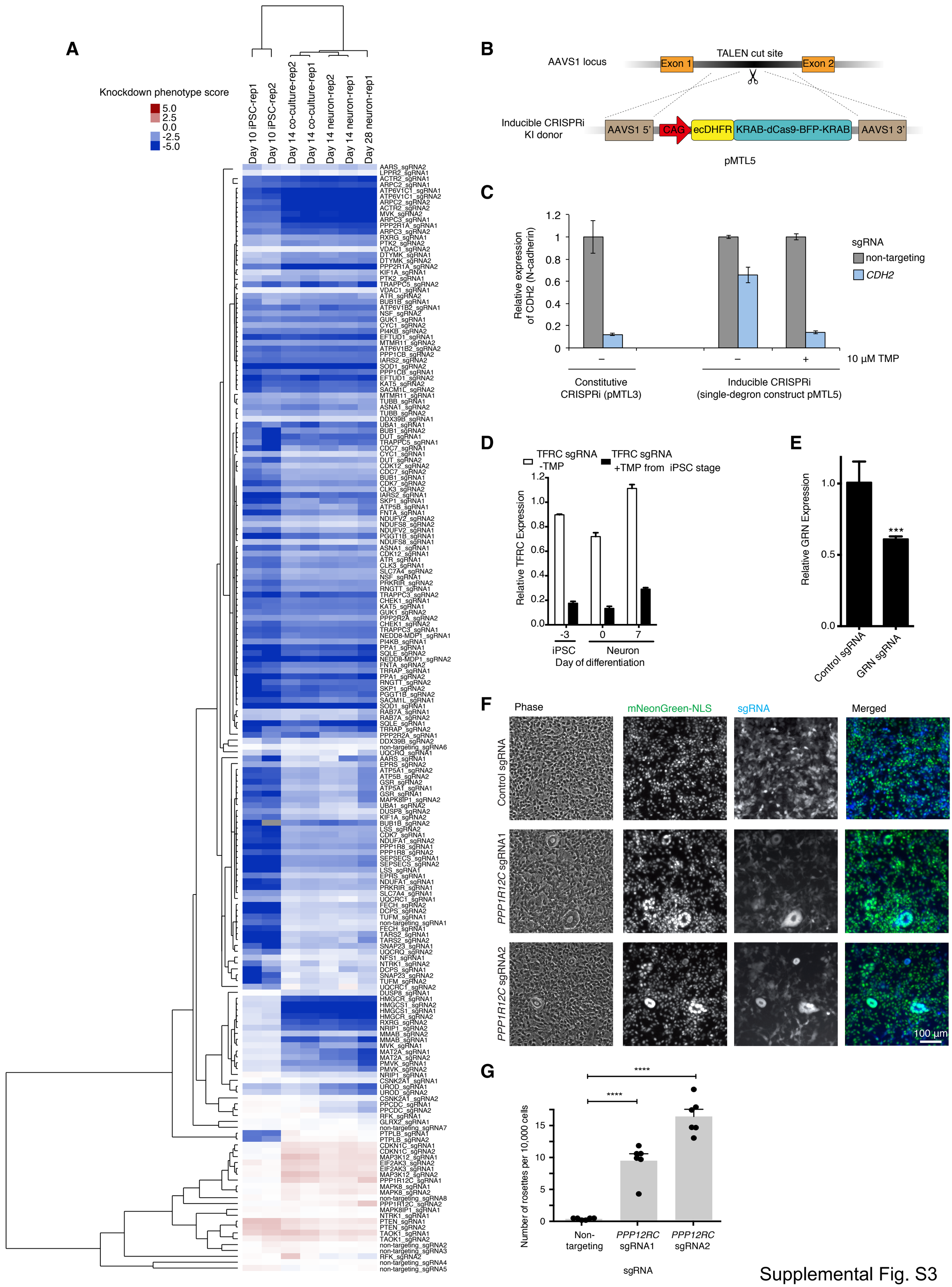

Supplemental Fig. S3

A

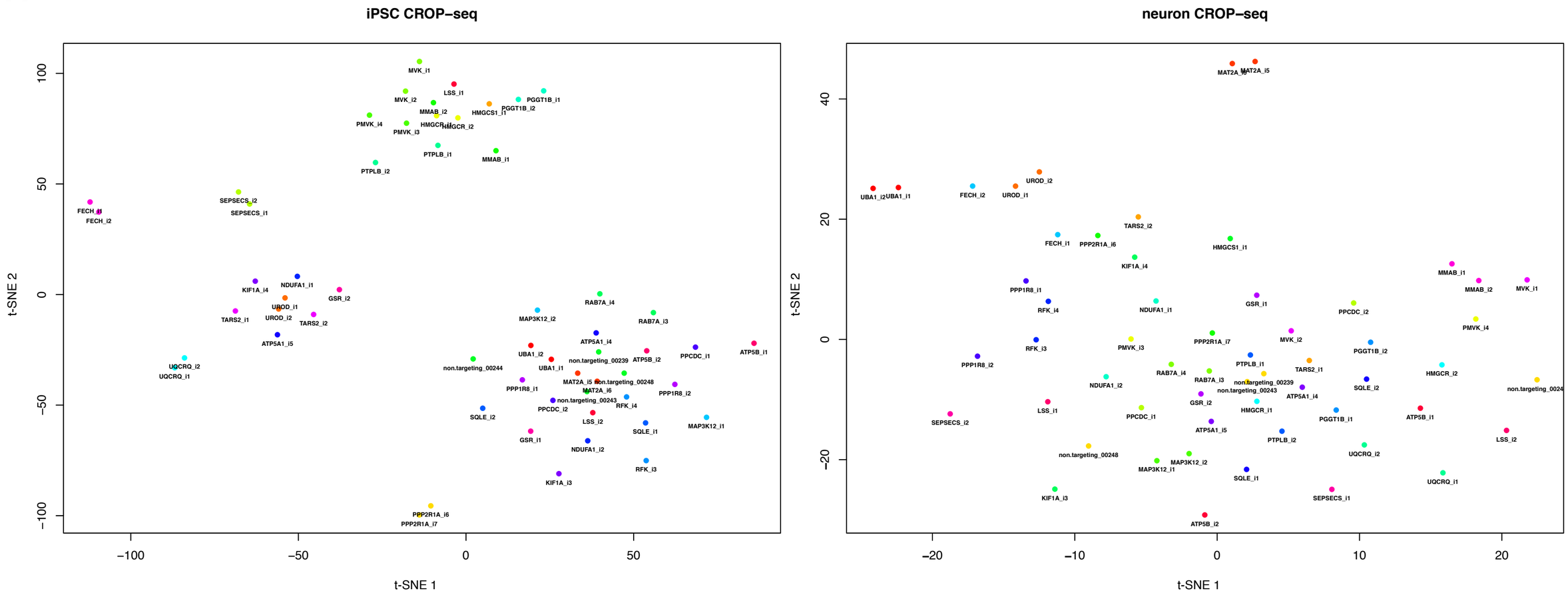

B

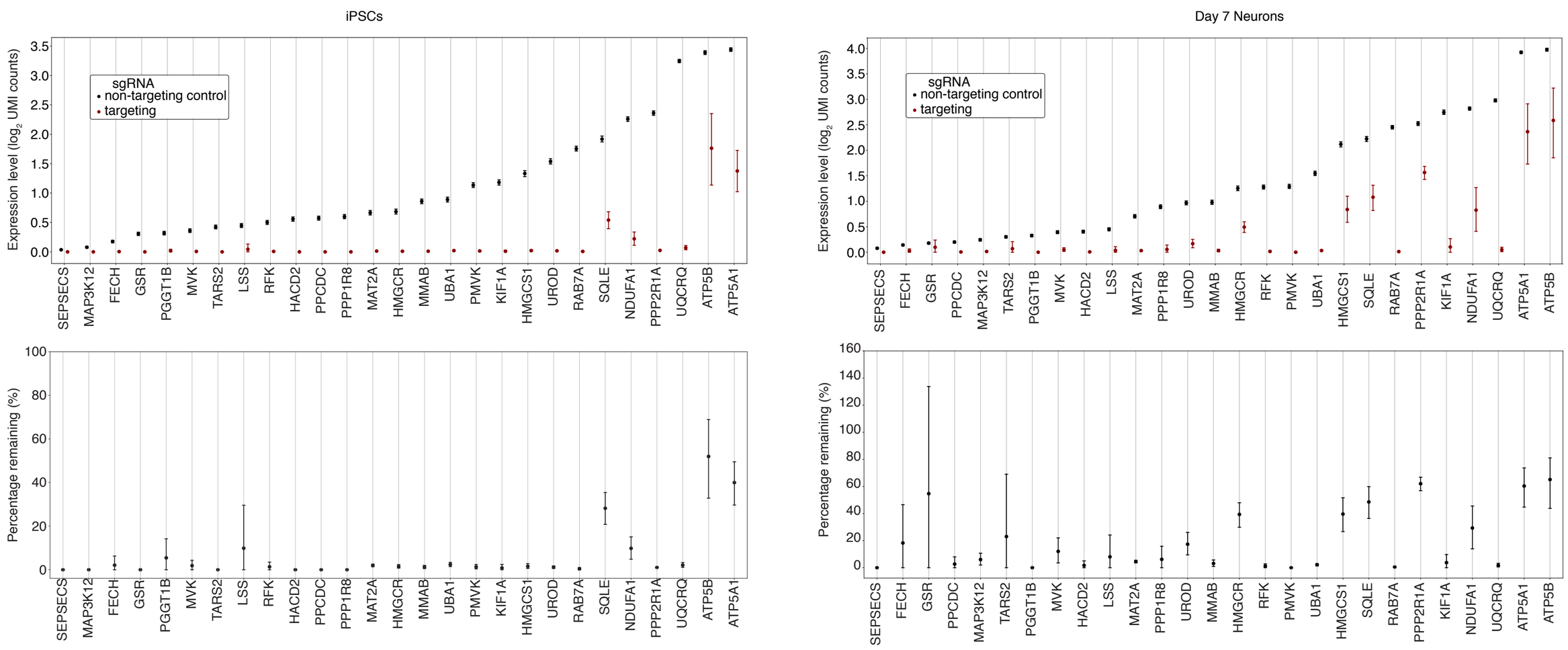

Supplemental Fig. S4

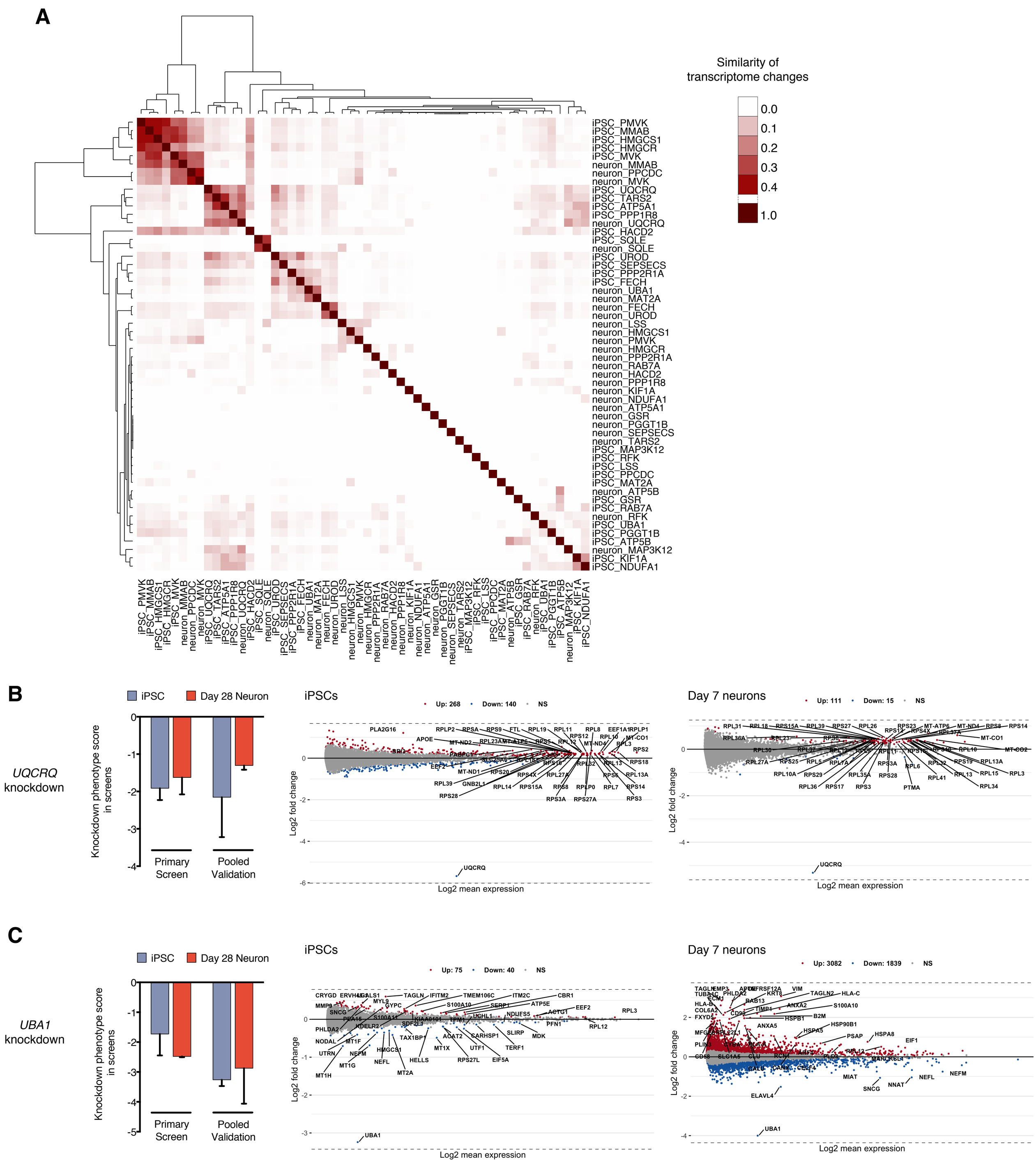

Supplemental Fig. S5
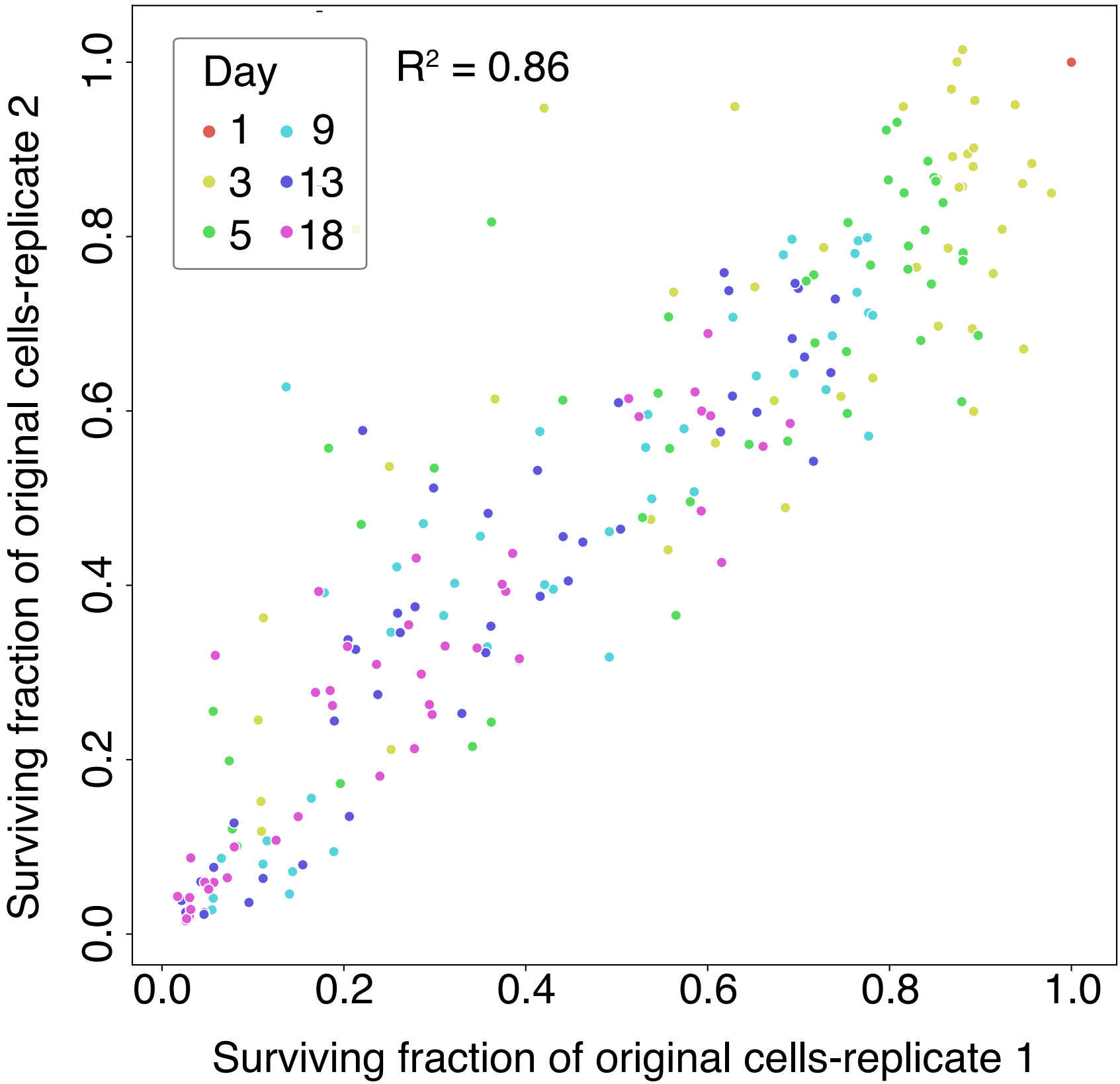
Supplemental Fig. S6